Technical Report Documentation Page

MTC Report Number: ME-84-01	ISBN Number:	Other Document Number:	Date: June 1984

Title: Signature Analysis of Radar Waveforms Taken on Asphalt-Covered Bridge Decks

Authors: T. Chung, C.R. Carter, McMaster University
D.G. Manning, F.B. Holt, MTC

Published by:

Research and Development Branch
Ministry of Transportation
and Communications

Client Group:

Participating Agencies:

McMaster University
Communications Research Laboratory

Abstract:

Research work by MTC has demonstrated the ability of ground-penetrating radar to detect deterioration in asphalt-covered bridge decks and to determine the thickness of the asphalt overlay. A single pass of the radar over the length of the deck generates two million bytes of data. Processing this vast amount of information rapidly required a microcomputer-based analysis program developed by the McMaster University Communications Research Laboratory. Using this program, the data can be analysed quickly and accurately to produce plans showing the location, extent and type of deterioration as well as the asphalt overlay thickness.

The report documents the objectives of the project, the existing analysis procedures, the radar waveform characteristics, and the operational characteristics of the computer programs. Recommendations for future research are also included.

Key Words: ground-penetrating radar, deterioration, asphalt-covered bridge decks, asphalt thickness, computer processing.

Comments: Study conducted under OJT & CRP project no. 22140.

Distribution: By request.

Copyright Status: Crown copyright.

ME-84-01

Signature Analysis of Radar Waveforms

T. Chung
Research Engineer
Communications Research Lab
McMaster University

C.R. Carter
Associate Professor
Dept. of Electrical and Computer Engineering
McMaster University

D.G. Manning
Principal Research Engineer

F.B. Holt
Research Technical Officer

Research and Development Branch, MTC

Published by:
Research and Development Branch
Ontario Ministry of Transportation and Communications
Hon. James W. Snow, Minister
H.F. Gilbert, Deputy Minister

Published without prejudice
as to the application of the findings.
Crown copyright reserved; however, this
document may be reproduced for non-commercial
purposes with attribution to the Ministry.

For additional copies write:
The Editor, Technical Publications
Ministry of Transportation and Communications
1201 Wilson Avenue
Downsview, Ontario
Canada M3M 1J8
(416) 248-7226
June 1984

TABLE OF CONTENTS

PAGE

List of Figures iii

Executive Summary iv

1/ INTRODUCTION 1
1.1/ Problem 1
1.2/ Objectives of The Project 1
1.3/ Overview of Existing Methods. 1
1.3.1/ Ontario Ministry of Transportation and Communications [1] . 1
1.3.2/ Georgia Institute of Technology [2] 2
1.3.3/ Alongi, Cantor et al [3]. 2
1.3.4/ The Port Authority of New York and New Jersey, and Cantor & Kneeter [4,5]. 3
1.4/ Methods of Analysis for this Project. 4

2/ SITE VISIT TO PAPINEAU CREEK BRIDGE 5
2.1/ Background. 5
2.2/ Measurements Made 5
2.3/ Analysis of the Data. 6

3/ METHODS OF WAVEFORM ANALYSIS 7
3.1/ An Heuristic Approach 7
3.2/ The Radar Signal Waveform 8
3.3/ Radar Waveforms Produced by Good Deck 8
3.4/ Radar Waveforms due to Scaling. 9
3.5/ Radar Waveforms due to Debonding. 10
3.6/ Radar Waveforms due to Delamination 10

4/ COMPUTER PROGRAMS AND RESULTS 11
4.1/ Dielectric Constant of Asphalt. 11
4.2/ Thickness of Asphalt. 12
4.3/ Debonding and Scaling 13
4.4/ Delaminations 14
4.5/ Field Testing 15

5/ COMPUTER SYSTEMS FOR PROCESSING THE DATA 17
5.1/ Strategy for Computer Processing of Radar Signals 17
5.2/ Sampling and Digitizing 18

6/ CONCLUSIONS AND RECOMMENDATIONS FOR FURTHER RESEARCH 21
6.1/ Conclusions 21
6.2/ Recommendations for Further Research. 21

REFERENCES 23

LIST OF FIGURES

PAGE

1/ Plan View of the Papineau Creek Bridge Showing Areas of Delamination, Scaling and Debonding. 25
2/ Transmission and Reflection of the Radar Signal from the Bridge Deck Structure. 26
3/ Signal Received from Good Bridge Deck. 26
4/ Radar Signal Waveform on Expanded Time Scale 27
5/ Overall Radar Waveform 28
6/ Radar Reflection from an Area of a Good Structure. 29
7/ Gated Video for a Region with No Defects 30
8/ High Video for a Region with Severe Scaling. 31
9/ Gated Video for a Region with Severe Scaling 32
10/ High Video for a Region with Debonding 33
11/ Gated Video for a Region with Debonding. 34
12/ High Video for a Region with Delamination. 35
13/ Gated Video for a Region with Delamination 36
14/ High Video Comparison. 37
15/ Gated Video Comparison 38
16/ Programs for Calculating Asphalt Thickness and Generating the Printout of Asphalt Thickness. 39
17/ Depth of Asphalt Printout. 40
18/ Waveforms Showing Scaling. 41
19/ Waveform Showing Debonding 42
20/ Plot of Ratio R1 and R2 for the B Line 43
21/ Plot of Ratio R1 and R2 for the B Line 44
22/ Plot of Ratio R1 and R2 for the B Line 45
23/ Flow Charts of Ratio Test and Zero Crossing Subroutine 46
24/ Areas of Debonding and Scaling 47
25/ Plot of the Bridge Deck Using the Ratio Test 48
26/ Plot of Sign Changes for the I Line. 49
27/ Plot of Sign Changes for the I Line. 50
28/ Plot of Sign Changes for the I Line. 51
29/ Plot of Areas of Delamination. 52
30/ Plot of Areas of Delamination. 53
31/ Papineau Creek Comparing the Actual Delaminated Areas with the Computer Results. 54
32/ Block Diagram of the Sampling and Digitizing System 55
33/ Frequency Response 56
34/ Transient Response 57
35/ Overall Block Diagram of the System. 58

EXECUTIVE SUMMARY

Objectives

The objectives of this study were to assess existing procedures for the analysis of radar waveforms; to identify those portions of the waveforms taken on asphalt-covered bridge decks which represent deterioration; and to develop a program capable of determining the thickness of pavement, recognizing types of deterioration and generating output in the form of a site plan showing areas and type of deterioration. Of central importance in this study was the use of real data collected on a bridge deck having known imperfections.

Methods Employed

A review of the existing literature indicated that time domain analysis has been used to great advantage in this type of work. After a brief attempt at using spectral analysis, it was concluded that time analysis did, in fact, provide the best chance for realizing the desired goals.

Radar measurements of the bridge deck at the Papineau Creek test site were recorded using an impulse radar having a pulse width of approximately 0.9 ns. The radar was mounted in a specially equipped monitor van developed by MTC personnel and driven over the bridge deck following grid lines spaced at half-metre intervals. The collected data were then processed using an HP 1000 minicomputer.

Strategy for Data Processing

After an evaluation of the data, it was found that the desired objectives could be realized by measuring the location and amplitude of the peak excursions of the video waveforms. In particular, it was found that the thickness of the asphalt could be measured accurately by determining the time delay between the first two positive peaks of the video waveform. This measurement is most useful when asphalt thickness exceeds 50 mm.

Further, it was noted that the ratios of amplitude-of-first-negative-peak to amplitude-of-first-positive-peak (R1) and amplitude-of-second-positive-peak to amplitude-of-first-positive-peak (R2) yielded parameters which were of considerable use in detecting scaling and debonding. For most of the bridge deck, it was found that the R1 values ranged from approximately 0.6 to 0.95 while the R2 values ranged from 0.05 to 0.4. In general, it was noted that the larger values of both R1 and R2 indicated scaling while large R2 and small R1 indicated debonding. Smaller values of R1 and R2 were usually indicative of good bridge deck. A computer model was developed which gave strong support to these experimentally determined results.

The problem of detecting delamination was solved by noting that the reflections from the asphalt-concrete interface and the top mat of reinforcing steel in the concrete are both well defined when no fault is present. When a fault occurs, however, the reflection from the top mat of steel is badly distorted resulting in a waveform which can easily be detected. This leads to a test based on waveform slope which counts the number of zero-crossings. Thus, the requirements of measuring asphalt thickness, detection of faults and plotting of data on a bridge deck layout are met.

Overall Results

It is concluded that the objectives of the project have been realized. In particular, it is seen that impulse radar is extremely useful in measuring asphalt thickness, especially when the thickness exceeds 50 mm. In addition, faults such as scaling, debonding and delamination can be located accurately using the computer techniques. For example, the Papineau Creek data set comprises approximately 25 million bytes of data. Using the computer and the specially developed algorithms, it was possible to reduce this to a set of plan views of the bridge deck. The first plan view shows the asphalt thickness to the nearest millimetre every metre (averaged over 10 cm intervals) along each line of the deck. The overall average asphalt thickness is also calculated. The remaining plan views of the bridge deck show the locations of areas of scaling and debonding and areas of delamination.

Since the locations of these faults were known, a comparison was made which showed that computer processing of the radar-generated data gives good estimates of actual fault location.

Finally, it was shown that a relatively simple microcomputer based system using the IBM-XT or equivalent and certain additional hardware packages would be capable of processing the data, albeit not in real time. This system would have many advantages over a mainframe computer or a mini-computer in areas such a flexibility and cost-effectiveness.

1/ INTRODUCTION

1.1/ Problem

Testing has demonstrated the capability of impulse radar to detect deterioration in concrete deck slabs which are covered with bituminous surfacing [1-5]. MTC currently defines areas of deterioration by manually examining a photograph of the radar waveform taken at specified grid points. A data reduction process is required which will recognize and interpret variations in the waveforms recorded continuously on magnetic tape.

1.2/ Objectives of the Project

The overall objective of the project was to produce a computer program and user guide for the analysis of radar waveforms from magnetic tape, with the output of the program in the form of a plan of the bridge deck showing areas and type of deterioration. The study involved the following tasks:

1/ Assess existing procedures for the analysis of radar waveforms.

2/ Identify those portions of the waveforms taken on asphalt-covered bridge decks which represent deterioration.

3/ Develop a program which will determine thickness of pavement, recognize types of deterioration and generate output in the form of a site plan showing areas and type of deterioration.

1.3/ Overview of Existing Methods

There has been some previous work published in the literature relating to the radar detection of faults in pavement and other similar structures. These are reviewed briefly in the following sections.

1.3.1/ Ontario Ministry of Transportation and Communications [1]

The study reported in Reference 1 evaluated the technical and economic factors of analysing the condition of bridge decks with bituminous surfacing. Methods examined included the chain drag, sonic reflection,

ultrasonic transmission, microseismology, resistivity, electrical potential, radar, and thermography.

Radar and thermography were found to have the most potential for the development of routine operational procedures. In particular, the radar proved very useful in measuring asphalt thickness and providing confirmation of the results obtained by thermography as to bridge deck condition.

1.3.2/ Georgia Institute of Technology [2]

This study [2] examined the feasibility of using pulsed radar for locating and measuring voids beneath reinforced and non-reinforced concrete pavements. The radar return signals from the structure were analysed on the basis of amplitude using a microcomputer. It was found that the location, depth and shape of the void could be determined by processing the radar signal. Unresolved problems were found to exist at high temperature and humidity; otherwise, the system performed well.

A significant finding was that for voids of less that two to three inches, the primary change was in the amplitude of the return signal. For voids of larger size, the time difference between signals was found useful. A superficial mathematical analysis was conducted however a number of factors were not taken into account.

1.3.3/ Alongi, Cantor et al [3]

This work describes in this report [3] involved the use of impulse radar as applied to the inspection of pavements such as highways, bridge decks, and runways. The study examined the change in reflected signal amplitude for reflections from pavements which have voids. A direct relationship was established showing how the delay between peaks in the reflected waveform can be used to determine void size. A further analysis related the various reflection coefficients and transmission coefficients as the signal propagated through the structure.

1.3.4/ The Port Authority of New York and New Jersey, and Cantor and Kneeter [4,5]

Impulse radar was used to evaluate bridge decks and the brick walls in tunnels. For the bridge decks, a van was outfitted with the radar and the return waveforms were recorded using a tape recorder. Runs were made of three bridges, namely Outerbridge Crossing, Bayonne Bridge, and George Washington Bridge. There was also an experimental evaluation made of the system using two concrete blocks separated by a gap. Measurements made on the bridge deck and in the laboratory both confirmed the usefulness of radar in detecting voids and measuring their size.

The measurements made on the tunnel were considered to be qualitative and not quantitative. Problems with large metal drainage pipes were not fully resolved.

The study reported in Reference 4 noted that cluster analysis can be used to advantage in grouping the data into classes. Essentially, the method depends on the plotting of the various parameters in n-dimensional space with the objective being to produce clouds of points having nearly like properties [6]. Then, decision boundaries can be generated and the number of points inside the various boundaries determined.

In the present application, cluster analysis would be useful if the expected locations of the clusters were known. Then, the locations of the clusters produced by the new data could be compared with the expected values to give an indication of the condition of the new bridge deck. It is also possible to use cluster analysis if the bridge deck is known to be mostly good. Then, the cloud of data containing the largest number of points would show where good bridge areas were located.

If the condition of the bridge deck is unknown, no such analysis is possible since the interpretation of the clusters is unclear. To base a decision on the variance of the locations of the points may also be dangerous. Note that in this case, it would be possible to mistake a deck which is entirely bad (due to one particular fault, say scaling) for one which is entirely good since cluster analysis might group the points into well defined regions in each case. Thus, cluster analysis was not investigated further in this study.

1.4/ Methods of Analysis for this Project

Two different methods of analysis providing useful information concerning the radar waveforms were identified. The first method relies on spectral estimation techniques using the Fast Fourier Transform (FFT) and the Maximum Entropy Method (MEM). The main advantage of these methods is that information can be obtained from waveforms when noise is present in the system. Certain features such as periodicities in the waveforms become apparent when the FFT and the MEM are calculated. Also, sharp transitions in the waveform are often detected when these methods are used.

The second method of analysis identified uses time domain processing. In this case, it is necessary that the waveform have a very low random noise content, especially for certain processes such as differencing. However, the method proved quite powerful in detecting amplitude variations and the location of certain events such as the time delay between two portions of well-defined events on a waveform.

For the present case, the time domain variations in the reflected signal related directly to the structure of the bridge deck (i.e., asphalt over concrete) and the type of fault. Further, the signal was almost without noise, permitting waveform feature analysis to be readily accomplished. Consequently, since time domain analysis applies directly to the received waveform and no advantage in noise suppression is possible using the FFT and MEM, it was concluded that the processing should proceed in the time domain. Thus, the main effort of the project focused on identifying techniques for best utilizing time domain processing.

2/ SITE VISIT TO PAPINEAU CREEK BRIDGE

2.1/ Background

The Papineau Creek Bridge, located near Bancroft Ontario, was selected for the test site [4]. The structure, built in 1968, has three spans and consists of a thin slab deck on prestressed concrete beams. It is approximately 37 m long and 9 m wide and typical of a large number of bridges in the Province. The bridge was built with an exposed concrete deck surface, and by 1980, the deck exhibited corrosion-induced distress. The condition of the structure was documented and a bituminous surfacing was placed without making repairs to the deck slab. A plan view showing the various faults is given in Figure 1.

A site visit was conducted to record radar signals from a specially equipped vehicle containing the radar, associated instrumentation packages and power generating facilities. Originally, it was intended that the signals would be recorded using the MTC tape recorder with a transfer of data being made to the Communications Research Laboratory (CRL) tape recorder. At the site, however, it was decided that the signals should be recorded directly using the CRL tape recorder.

2.2/ Measurements Made

The bridge deck was prepared for testing by marking off the deck surface with a 0.5 m grid. Three different types of measurements were made on site. The first was a set of spot recordings at selected locations which exhibited various known types of deterioration. This also included a measurement from a metal plate to allow calibration of the reflected waves and a measurement from the joint between the roadway and the bridge deck. It is thought that it may be possible to identify the joint, which would be extremely valuable in identifying the beginning of the bridge deck while in motion.

The second type of measurements included a complete set of runs from the south end of the bridge to the north end along each of the lettered grid lines marked on the deck (see Figure 1). Every measurement commenced with the mobile platform being positioned over the joint. This established a benchmark reference for all the runs. The vehicle speed over

most of the run was kept between approximately 3.5 and 5 km/h and every effort was made to ensure that the radar horn remained close to the line on the road. For the J-line (centreline) only, a set of three runs was made at speeds of 3.5, 7.2 and 11 km/h in order to determine effects of speed of the recorded waveforms.

The third type of measurement involved the use of orthogonal polarization. This was achieved by rotating the antenna 90° so that the E-field was at right angles to the direction of travel. It was expected that this might give some additional information in cases where the reflections are produced by structures with directional properties (such as reinforcing rods and the joint between roadway and bridge deck).

2.3/ Analysis of the Data

It was decided that the Papineau Creek data would form the data set for analysis of radar waveforms for this contract. In addition, it was further specified that the data with polarization parallel to direction of travel would be analysed at the nominal speed of 3.5 km/h. Although this is a subset of the total data taken, it was concluded that many important problems would be studied by dealing in depth with this data set. Thus, the remaining sections of the report will discuss the results of processing these data.

3/ METHODS OF WAVEFORM ANALYSIS

3.1/ An Heuristic Approach

It is possible to gain some insight as to the type of waveforms to be expected by simply considering the transmission and reflection of waves from the various layers of asphalt, concrete, rebars and air. For example, consider the structure of Figure 2 comprising air above asphalt, above concrete, above rebars. The incident wave falling on the air-asphalt interface is partially reflected with a reflection coefficient of -0.33, based on a dielectric constant for asphalt of 4, and partially transmitted with a transmission coefficient of 0.67. The wave proceeds through the asphalt, 80 mm in this case, to the asphalt-concrete interface where again the wave is reflected with a reflection coefficient of -0.105, based on a dielectric constant for concrete of 6.1, and transmitted with a transmission coefficient of 0.895. Note that the transmission coefficient is quite high in this case. Finally, the wave reflects off the rebars, assumed to be 50 mm below the concrete surface, with a negative reflection coefficient of relatively large but unknown value.

The resulting waveforms are shown in Figure 3 where we see that the surface reflection from the asphalt-air interface, the asphalt-concrete interface, and the rebars all have the same orientation, namely, 180° out of phase with the incident electric field. Adding the three waveforms together leads to the composite waveform shown which has the initial peak at A, from the asphalt, the second peak at C, from the concrete, and the third peak at D, from the rebars. Note that the time delay from peak A to peak C is a measure of the thickness of the asphalt and the time delay between peak C and peak D is a measure of the thickness of concrete over the rebars. This leads to the observation that a W shape occurs between the peaks at C and D due to the high value of the transmission coefficient, the structure of the signal, and the distance between the concrete surface and the rebars.

The three faults being considered in this project include debonding, scaling and delamination. Since debonding affects the interface between

the asphalt and the concrete, it is clear that the reflection coefficient between asphalt and concrete will no longer be -0.105. Unfortunately, the analysis is not trivial, but the overall result leads to a reflection coefficient with increased amplitude related to the dielectric constant of asphalt, air and concrete and the width of the gap. This can be calculated by using a Smith chart or a transmission line model. A similar effect takes place due to scaling since scaling occurs in the same region between asphalt and solid concrete.

Delamination occurs in the region between the surface of the concrete and the first layer of rebars. Essentially, a shallow crack develops in the concrete which leads to a discontinuity between the surface and the rebars. It can thus be postulated that if delamination is present, there will be distortion of the W shape since the crack will produce an additional reflection resulting in a far more complex reflected waveform. The results of this heuristic approach were compared with actual waveforms obtained.

3.2/ The Radar Signal Waveform

Two plots of the radar waveforms are shown in Figures 4 and 5 with the only difference being in the scale of the time axes. The waveform was obtained by positioning the radar antenna directly over an aluminum plate placed on the ground. We see from Figure 4 that the signal has a duration of approximately 0.9 ms between negative peaks P and Q with the main positive peak at A. The peak at A represents, in fact, the surface reflection from the aluminum plate. Also, the response after point R is very small, indicating that variations due to discontinuities can be detected in this region without too much interference. In the 'overshoot' region from Q to R, however, there exists a problem in detection since any defects near the surface will produce an interference pattern with this overshoot.

3.3/ Radar Waveforms Produced by Good Deck

The radar waveforms for a bridge deck in good condition are illustrated in Figures 6 and 7, for high video and gated video, respectively. The

peaks at B and C are well defined. The peak at A represents the surface reflection from the asphalt and the peak at C indicates the reflection from the asphalt-concrete interface. Measuring the time delay from peak C to peak A provides a measure of the thickness of the asphalt. Certain difficulties may arise when the asphalt is much less than 50 mm in depth if only simple computer analysis is applied. There is, however, a strong possibility that pulse cancellation techniques can be applied to greatly reduce this problem. Where the thickness exceeds 60 mm (as is the case for most bridge decks in Ontario) there should be little trouble in evaluating this depth.

A program has been prepared to automatically measure the asphalt thickness. The program, described in Section 4, first measures the dielectric constant of the asphalt and then determines average thickness over one metre segments and the overall average thickness.

The region from C to D is of special interest since the characteristic W predicted in Section 3.1 is clearly demonstrated for the case where the concrete surface is good. When delamination occurs in this region, the W becomes distorted, as detailed in Section 3.6.

3.4/ Radar Waveforms due to Scaling

Scaling occurs in the region between the asphalt and the concrete. Essentially, the concrete breaks down into a matrix of sand and coarse aggregate which may or may not contain water. If the matrix contains water, the dielectric constant will be substantially higher than either concrete or asphalt, producing a strong reflection. If the matrix does not contain water, there will also be a strong reflection since there will be an asphalt-air-concrete structure in which the dielectric constant of air is much lower than either of the other two materials.

Waveforms showing areas of severe scaling are illustrated in Figure 8 for high video and Figure 9 for gated video. Comparing Figures 6 and 8, we see that scaling produces spectacular change in the peaks at point B and point C. Furthermore, the waveform following point C appears to die out rather quickly as is seen in the gated video of Figure 9.

3.5/ Radar Waveforms due to Debonding

Debonding is caused by the asphalt lifting off the concrete base. The size of the gap between the asphalt and the concrete may be very small. It is expected that the waveform in the region of point C will be strongly influenced by debonding.

The video waveforms produced by debonding are very similar to those produced by scaling, differing mainly in degree. Figures 10 and 11 show the effects for high and gated video, respectively. It is seen that the levels at B and C are considerably higher than those obtained from a good bridge deck and yet not as high as those obtained from scaling. For very thin gaps between the asphalt and the concrete, there is a considerable increase in the amplitudes at points B and C relative to point A. However, it is noted that the loss factor in asphalt tends to mask the effect to some extent. Further work in this area is required in order to fully understand the process.

3.6/ Radar Waveforms due to Delamination

Delamination occurs in the region between the surface of the concrete and the first layer of rebars. As stated above, a shallow crack develops in the concrete which leads to a discontinuity between the concrete surface and the rebars.

Figures 12 and 13 show the waveforms obtained due to delamination. Figure 14 indicates that with delamination no large change in the high video takes place between points A and C. The gated video waveforms appear to have a large variation, however, as is seen in Figure 15. The trace between points C and D in each case for the delaminated areas is badly distorted as compared to the good areas and the characteristic W is poorly defined or absent.

Finally, it is observed that the traces for gated video all have the same general shape after point D. Thus, it is unlikely that any information can be gained from processing this part of the trace. In addition, the main area of interest lies in the first 50 mm of concrete. Hence, the processing should consider the waveform passing through the asphalt and just the first 50 mm of depth into the concrete.

4/ COMPUTER PROGRAMS AND RESULTS

4.1/ Dielectric Constant of Asphalt

The dielectric constant, relative permittivity of asphalt, must be measured in order that certain parameters can be calculated. This can be done by first recording the waveforms produced by the flat plate measurement described in Section 3.2 noting that the peak voltage is A1. Next, a recording of the waveform produced by an area of good pavement is made as shown in Figure 6. Again, we see that the surface reflection from asphalt is represented by the peak at A. This peak can easily be measured as voltage of amplitude A2. We note that the magnitude of the reflection coefficient is calculated as a ratio.

$$\rho = \left[\frac{A2}{A1}\right]$$

Once the value of ρ is determined, it is an easy matter to calculate the dielectric constant since the dielectric constant is given by:

$$\varepsilon_R = \left[\frac{1 + \rho}{1 - \rho}\right]^2$$

For the amplitudes obtained from measurements, it was found that the value of ε_R varied from approximately 3.9 to 4.1. Thus, the value used in the following calculations is 4.0. It is noted that two strategies could be used here. The first is to calculate the value of ε_R for each radar waveform. This is a good procedure when the composition of the asphalt is known to vary from area to area. The second strategy is to find the average value for ε_R and use this value for all calculations. This method is satisfactory for cases where the asphalt is relatively uniform and reduces the variation in the calculation. This was the method chosen for the calculations.

There are certain assumptions made in measuring the dielectric constant of the asphalt. First, and most important, it is assumed that the thickness of the asphalt is sufficient that the reflection is determined mainly from the asphalt alone and is not influenced by the material below. This will be true if the asphalt is at least half a wavelength

thick. Since the dielectric constant is of the order of 4, the corresponding asphalt thickness is 75 mm. Second, it is assumed that the asphalt is uniform in composition and behaves in an isotropic manner. Third, it is assumed that the asphalt is linear, i.e., doubling the electric field automatically doubles the magnetic field. Fourth, it is assumed that no hysteresis exists in the asphalt. Normally, this is true for all non-magnetic materials. Finally, it is assumed that the dielectric constant of the asphalt is time-invarient.

4.2/ Thickness of Asphalt

The thickness of asphalt can be determined by measuring the number of samples N between the surface reflection and the reflection from the asphalt-concrete boundary. Then, the thickness is given by the formula

$$\text{THICKNESS} = \frac{6N}{\sqrt{\varepsilon_R}}$$

It is assumed that the thickness of the asphalt is sufficiently large enough to prevent interference between the surface reflection and the reflection from the asphalt-concrete interface. This will normally be true if the asphalt is at least 50 mm thick. It is further assumed that if there is damage to the region between the asphalt and the concrete, there will still be a reflection produced which will allow the thickness measurement. Normally, this is true; however, the actual measurement may be in error by any amount depending on the damage.

A computer program has been written for calculating the asphalt thickness. The flowchart is illustrated in Figure 16a. Once the data are entered into the computer as data files, the amplitudes A1 and A2 are measured using program DEPTH. Then, the ratio is taken in order to calculate the reflection coefficient. The reflection coefficient can then be used to find the dielectric constant.

For the remaining data, the time delay is measured using the main program. The thickness is determined for each location selected by the fifth wheel. These different measurements are then averaged over a one metre interval and the results are stored. As well, the average for an

entire line is determined since it is desired to find the overall average depth of the asphalt. This concludes program DEPTH.

The next step is to generate the table used to produce the plot of depth for the entire bridge deck using program TABLE (Figure 16b). A sample of the output produced on the line printer is given in Figure 17. Here we see that the depth is given in millimetres with the average depth of each line being provided at the bottom of the chart along with the overall average depth. Although this plot is provided by a line printer, there is no reason that the information could not be printed using a plotter.

4.3/ Debonding and Scaling

Debonding and scaling are detected by using a ratio test based on the amplitude of the signal at point B divided by the amplitude at point A (R1 = B/A) and the amplitude of the signal at point C divided by the amplitude at point A (R2 = C/A). Normally the R1 and R2 ratios are approximately 0.7 and 0.12, respectively, for a good bridge deck. However, the ratios are uniformly high when scaling occurs. For scaling, the R1 ratio is close to one and the R2 ratio is above 0.35, as shown in Figure 18. For debonding, the R1 ratio is close to normal but the R2 ratio is considerably higher than normal, as illustrated in Figure 19. A set of plots for the two ratios taken on the B line is shown in Figures 20, 21 and 22. The regions of scaling and debonding are indicated.

A subroutine for automatically determining the R1 and R2 ratios has been developed. The flowchart is illustrated in Figure 23a. Essentially, the data entering the computer are scanned to locate the peak at A for each waveform. Then, the peaks at B and C are located and the two amplitudes are measured. This permits the calculation of the two ratios R1 and R2 and the time delay between peaks for the asphalt thickness measurement. A plot of good and bad locations on the Papineau Creek bridge is given in Figure 24. The areas marked with **X** represent scaling while the areas marked with **O** are debonded. Note that there is close agreement with the observed bridge condition shown in Figure 1.

The possibility of detecting the ends of the bridge deck also exists using the R1 and R2 ratios. It was noted that both ratios become very

large over the joint between the roadway and the deck. However, the possibility of mistaking this for scaling can easily occur. Thus, it is suggested that, if possible, the ends of the deck be noted using the observation of the operator.

4.4/ Delaminations

Since delamination occurs in the region beyond C, the R1 and R2 ratio tests are of little value. This is in fact confirmed by the plot of Figure 25. The ratios have been selected on the following basis: R1 is examined to ensure that it is near 0.65 while a fault is declared when R2 falls below 0.12. As can be seen, there are large areas of delamination which are not detected.

A second method of detecting delaminations was developed based on the waveform between points C and D (see Figures 6 and 12 for good and delaminated traces, respectively). Here, it has been noted that the characteristic W occurs when the structure is good but the W becomes distorted when delamination occurs. The subroutine OXING for calculating this shape (Figure 23b) is based on counting the number of slope sign changes between points C and D. If the number of sign changes is two, then the structure is bad. If the number of sign changes is three or four, then the structure is good. A plot of the sign changes for the I-line is given in Figures 26, 27 and 28. We see that delamination occurs at both ends of the line and in regions near the 10-13, 24-26 and 29-31 metre ranges which is in close agreement with Figure 1.

A plot of the whole bridge deck showing delaminations is given in Figure 29. Figure 30 illustrates the reduction in fault detections which takes place when the single-hit indications are eliminated. An overlay has been prepared, as shown in Figure 31, which compares Figure 1 with the delaminations detected by radar (Figure 30). The agreement is reasonably good.

4.5/ Field Testing

The above material indicates how the measurements of asphalt thickness and dielectric constant can be obtained, and how a computer may be employed to process the data. From an operational standpoint, there are some procedures which may further enhance the performance of the system.

Firstly, it should be possible to determine beforehand what type of asphalt is used on a specific bridge deck. This would give some information as to the expected waveforms which should to obtained, especially from the surface reflection. As well, it would be possible to determine the approximate range of values which should be obtained for R1 and R2. If the computer is in the field, these could be stored in memory and a correlation calculated to determine whether the signal in question is sufficiently close to the expected waveform. If the computer is not in the field, it would be possible to generate expected waveforms beforehand. In either case, the asphalt thickness measurement and the dielectric constant measurement could be compared with expected waveforms and any great discrepancy could be investigated prior to the taking of large amounts of data. This is important since all the asphalt thickness measurements depend on these two records.

Secondly, it would be valuable to record any additional information about the bridge deck which would aid in the processing of the data. This would include information about location of the joints in the deck and any cracks or other physical features which may be apparent.

Thirdly, it is important to note the various environmental factors such as temperature and any recent rainfall (which may produce water in regions between the asphalt and concrete).

Finally, if real time processing is performed in the field, it would be possible to use stored R1 and R2 values to give an indication on-site as to the condition of the bridge deck. The obvious advantages of this include:

- First, the confirmation of a valid data set. Data may be invalid due to environmental factors, equipment failures or operating procedures.

- Second, the status of the bridge deck is evaluated immediately so that further measurements may be taken if desired. This is particularly useful if the computer indicates a very bad deck.

- Third, it may be unnecessary to accumulate large amounts of raw data. However, there is a serious problem which should be considered and this relates to using the computer in a mobile vehicle. Normally, disc drives should not be used while in motion. Hence, it may be necessary to stop the vehicle before running the computer. This would lead to the accumulation of data using either the tape recorder or possibly the RAM memory of the computer.

5/ COMPUTER SYSTEMS FOR PROCESSING THE DATA

5.1/ Strategy for Computer Processing of Radar Signals

The modern microcomputer appears to be the ideal choice for processing the radar data. Reasons for this include:

- The initial cost of a microcomputer is one order of magnitude ($15 000) less than a minicomputer ($100 000) and two orders of magnitude less than a mainframe ($1 million and up). Thus, it is cost-effective.

- Inputting the data to the microcomputer is very simple since interface cards now exist at reasonable cost which are fully capable of handling the speeds required. Furthermore, it is a simple matter to include monitoring functions to ensure the data are being properly loaded into the computer.

- The processing speed of the microcomputer is well matched to the data rate coming from the tape recorder. Thus, it appears very likely that some processing could be done in real time directly off the tape recorder.

- The need for a special operator is eliminated since most microcomputers are user friendly. Thus, the personnel operating the radar and the tape recorder can also operate the microcomputer. This usually has an enormous advantage since the whole process is controlled by the same people.

- The microcomputer program is easily modified and adapted to any changing conditions. The capability exists for loading floppy discs with special processes which are developed by other researchers.

- Large memory is now available in both the computer (solid state RAM) and externals (in the form of magnetic discs). This is of great importance in this project since there is a huge data file to be processed for each bridge deck. Ideally, an entire bridge deck would be loaded into the disc storage in order to allow the simplest procedure and the fastest processing time.

- The microcomputer and its peripherals are portable. Consequently, the possibility of processing in the field is quite good. This may be of considerable benefit in remote sites since the data could be processed on location. Any problems would be detected immediately, thus eliminating a return visit which would be time-consuming and costly.

5.2/ Sampling and Digitizing

A block diagram of a sampling and digitizing system which can be used to interface the tape recorded signals to the microcomputer is illustrated in Figure 32. The first input is the high video, which gives the overall trace. This video is normally used for analysing the signals. The second input is the gated video, which is used to provide a more detailed picture of the waveform following the surface reflection. If a sufficiently precise analog-to-digital converter is used, then the gated video input may not be required. The input voltage level is bipolar (positive and negative) and never greater than 2 V in amplitude. Assuming that the minimum detectable signal would be no smaller than 4 mV, then it is clear that a 10 bit analog-to-digital converter would be capable of handling the digitization. Since some margin would be desirable, the choice of a 12 bit converter would not be unwise provided that the additional cost is reasonable.

The third input is the fifth wheel data which are used to measure distance. This input may be in one of two forms. First, the raw data from the fifth wheel could be fed to the computer and processed in order to obtain the distance information. The output from the fifth wheel is at logic levels and one pulse corresponds to a distance of 10 cm. Second, the distance data are processed using a digital interface which counts the fifth wheel pulses and converts them into four bytes of data representing distance every half metre. This data source is available in both serial format and parallel format. In either case, the signal would enter the computer through a digital port.

Initial measurements indicated that the bandwidth of the radar waveforms is well below the frequency of 5000 Hz. Consequently, it is desirable that Butterworth lowpass filters having a 3 dB bandwidth of 5000 Hz be used at the input to the two analog channels. The frequency response curve of the filters is shown in Figure 33 and the transient response is illustrated in Figure 34. It is seen that the response at 10 000 Hz is approximately 18 dB down with respect to low frequency. Thus, a sampling rate of 25 000 samples per second would be suitable for the analog-to-digital converters. The transient response curve indicates that there is very little 'ringing', which is a highly desirable feature.

The filters feed directly into the sample-and-hold amplifiers which are at the input to the interface board of the microcomputer. The analog-to-digital converters then digitize the signal and allow the computer to store the signal either in computer memory or on the disc.

Commercially available interface boards can now be purchased which will provide the necessary input to the computer. Note that a sufficiently high sampling rate (> 27.5 kHz) is required. It is necessary to use a Butterworth filter at the input to the board in order to assure proper sampling performance.

An overall block diagram of the processing system is shown in Figure 35. In normal operation, the operator would first initialize the computer to await the input from the tape recorder. Once initialized, the operator would start the tape recorder and the computer would read the data. Two different inputs must be considered:

- first, the digitized video at a rate of approximately 25 000 samples per second, and
- second, the fifth wheel input occurring at a much lower rate.

Assuming two bytes per digitized video sample the hard disc would be capable of storing a total of about 200 seconds of data at one time.

Note that the fifth wheel input is so slow in comparison to the video input (perhaps 10 to 20 times per second) that it can essentially be ignored from a capacity standpoint. The method described above assumes

that the data will first be loaded onto the disc prior to processing. There is a second possibility in which the data may be processed as soon as it enters the computer. It has not been determined whether or not this is possible. It would depend mainly on the time required to run the 'input data' routine.

6/ CONCLUSIONS AND RECOMMENDATIONS FOR FURTHER RESEARCH

6.1/ Conclusions

It is concluded that:

- Impulse radar can be used to accurately detect faults in bridge decks.
- Faults such as scaling, debonding and delamination can be identified using computer techniques.
- Thickness of asphalt can be measured. However, a problem arises when the asphalt thickness is less than approximately 50 mm.
- Automatic processing of the waveforms is not only possible, it is also desirable in that the amount of data can greatly be reduced and a uniform criterion can be employed to detect faults.
- A microcomputer is well suited for processing the radar data. It is highly desirable to use a hard disc with at least 10 megabytes for storage.
- A preliminary study has shown that modelling of the waveforms gives valuable insight to the behaviour of the reflections obtained.

6.2/ Recommendations for Further Research

It is recommended that:

1/ An investigation be conducted to determine the capability of the system for an array of different asphalt mix types and different bridge deck structures such as asphalt over concrete, concrete overlays, and exposed concrete. This could lead to a set of standard characteristics which would categorize a large number of bridge decks.

2/ An assembly language program be developed which would greatly speed the data processing by eliminating the redundancies of high level language.

3/ A realistic model be developed which would aid in classifying the different forms of deterioration.

4/ The problem of vehicle speed and wave polarization be studied in more detail.

5/ The effects of steel bars in concrete on the radar waveform be further investigated.

7/ REFERENCES

[1] Manning, D.G. and Holt, F.B., "Detecting Deterioration in Asphalt-Covered Bridge Decks," Transportation Research Record 899, TRB, Washington, D.C., January 1983, pp. 10-20.

[2] Steinway, J.W. et al, "Locating Voids Beneath Pavement Using Pulsed Electromagnetic Waves," National Research Council, Washington, D.C., November 1981.

[3] Alongi, A.V. et al, "Concrete Evaluation by Radar Theoretical Analysis," Transportation Research Record 853, pp. 31-37 (1982).

[4] Cantor, T.R. and Kneeter, C.P., "Radar as Applied to Evaluation of Bridge Decks," Transportation Research Record 853, pp. 37-42 (1982).

[5] Cantor, T.R. and Kneeter, C.P., "Radar and Acoustic Emission Applied to the Study of Bridge Decks, Suspension Cables and a Masonry Tunnel," The Port Authority of New York and New Jersey, Engineering Department, Research and Development Division, Report No. 77-13, December 1977.

[6] Duda, R.O. and Hart, P.E., Pattern Classification and Scene Analysis, John Wiley and Sons (1973), pp. 189-260.

FIGURES

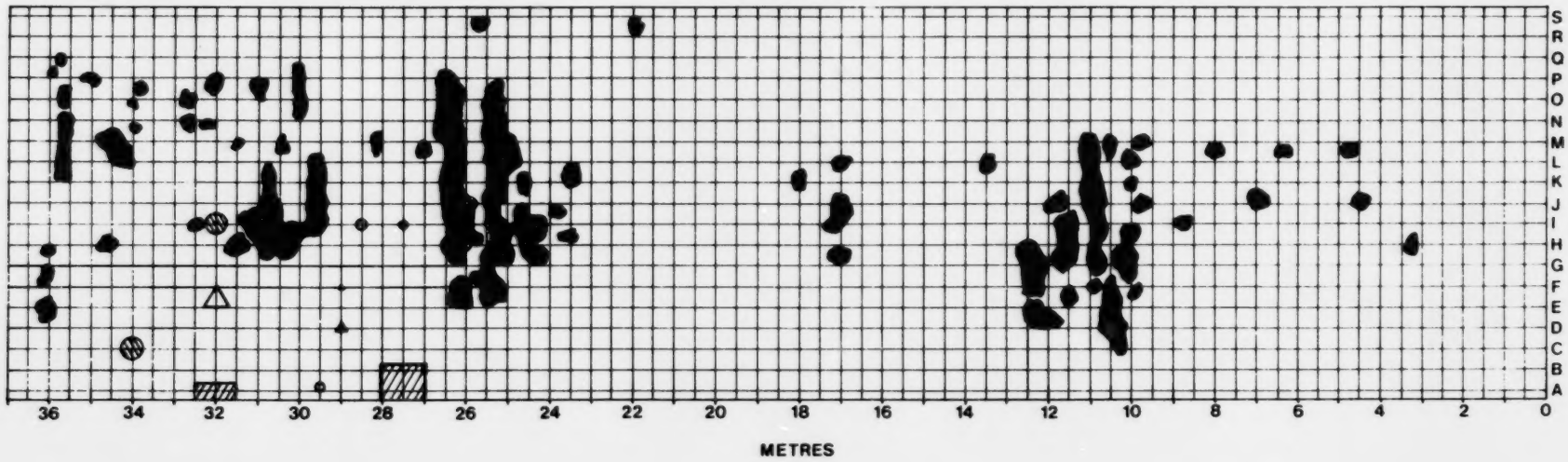

Figure 1/ Plan View of the Papineau Creek Bridge Showing Areas of Delamination, Scaling and Debonding

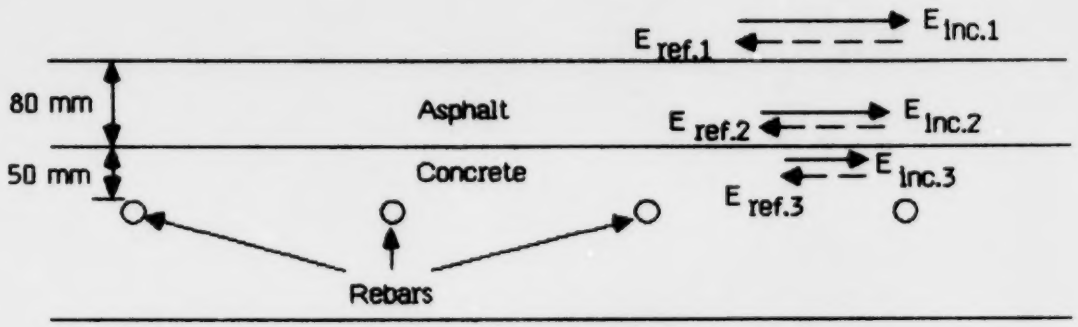

Figure 2/ Transmission and Reflection of the Radar Signal from the Bridge Deck Structure
Note that the Reflected Waves are all 180° out of Phase with the Incident Waves.

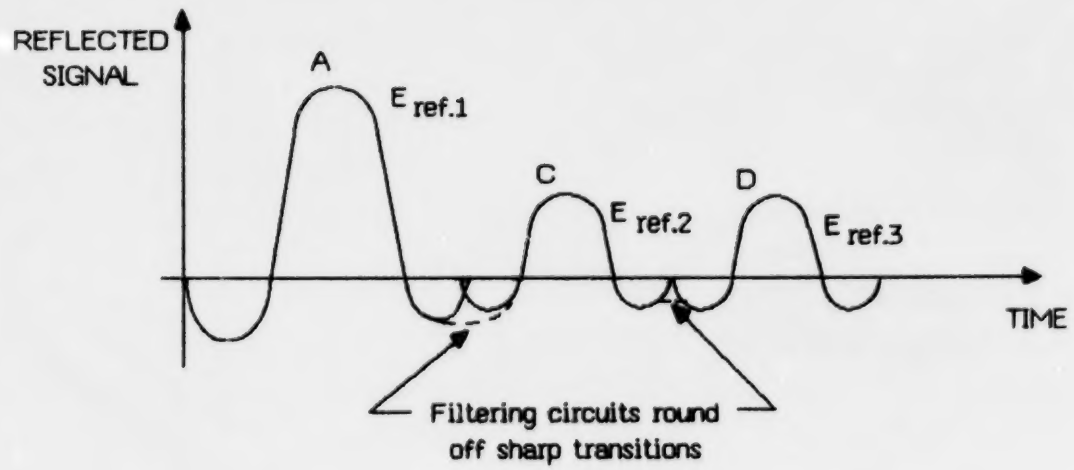

Figure 3/ Signal Received from Good Bridge Deck
Note the Peaks at A,C and D are all well defined and the Characteristics W between C and D.

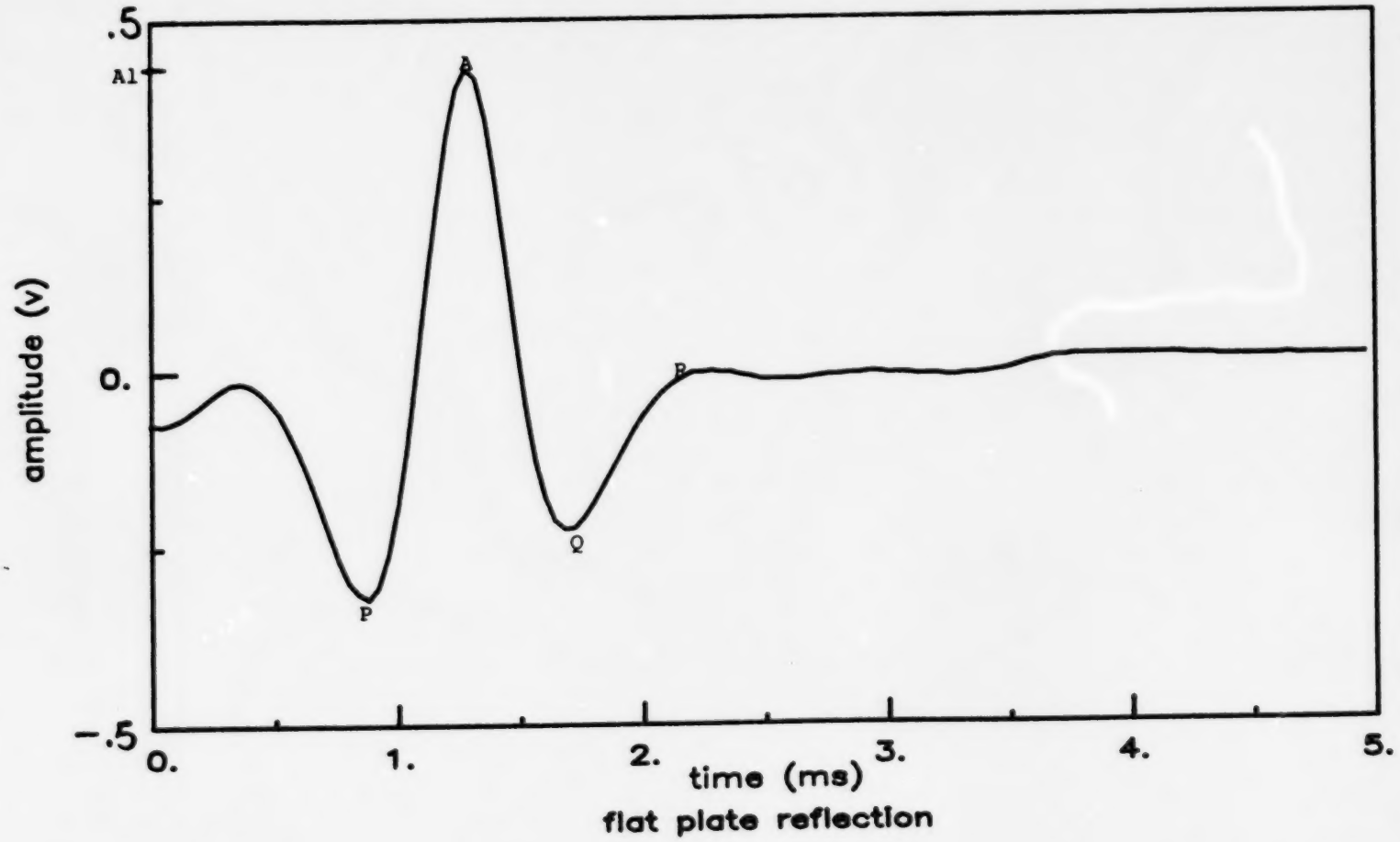

Figure 4/ Radar Signal Waveform on Expanded Time Scale

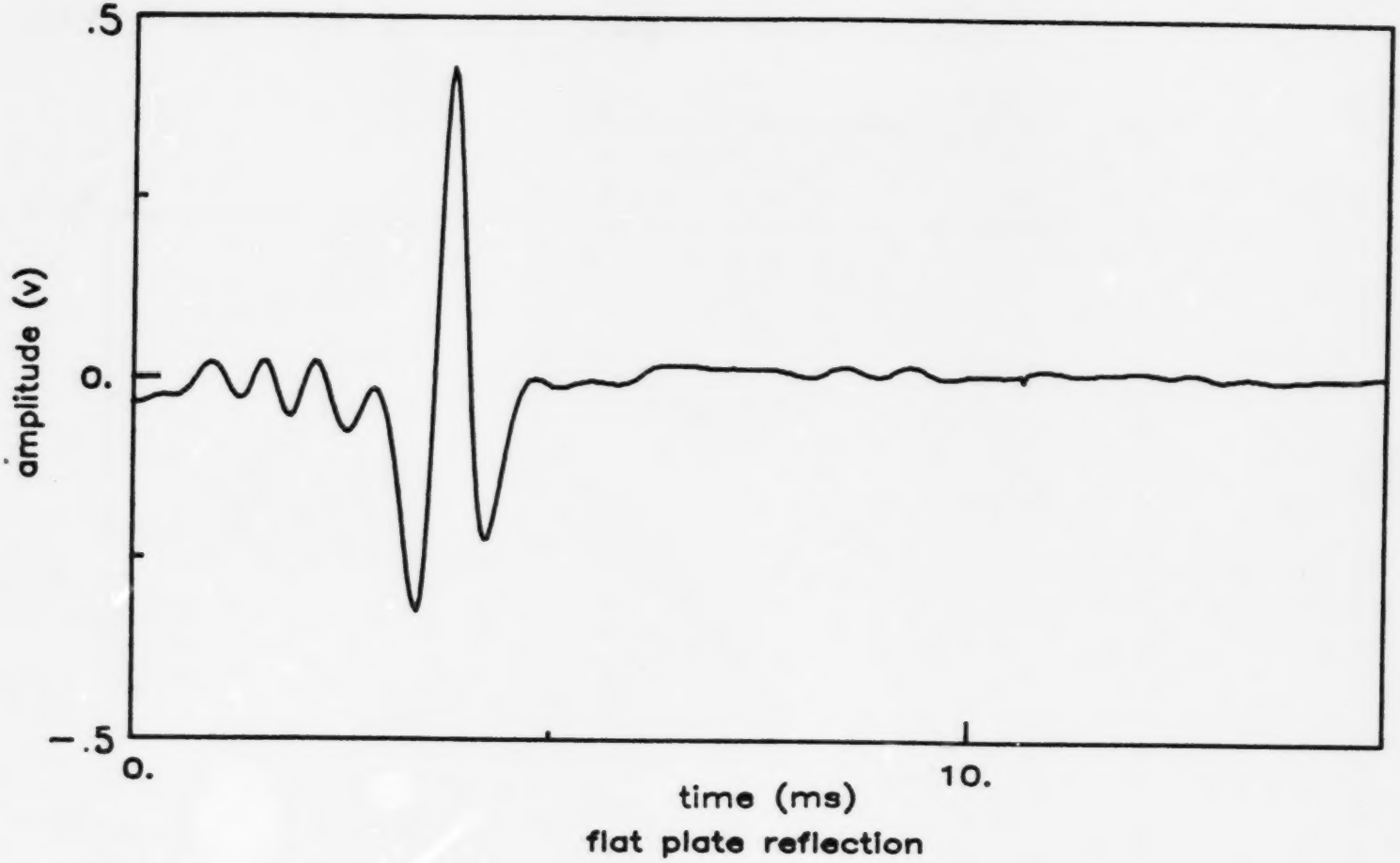

Figure 5/ Overall Radar Waveform

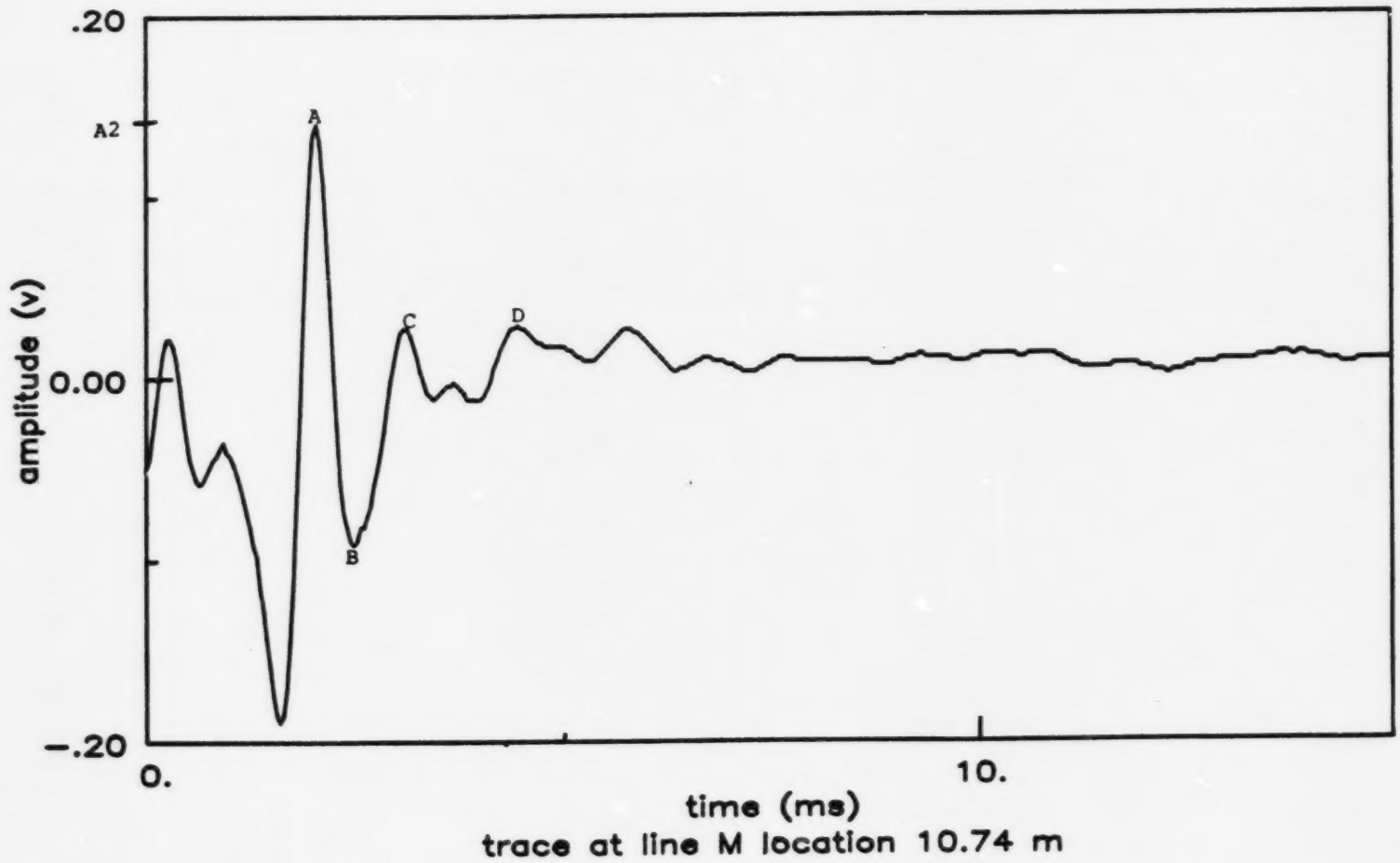

Figure 6/ Radar Reflection from an Area of Good Structure

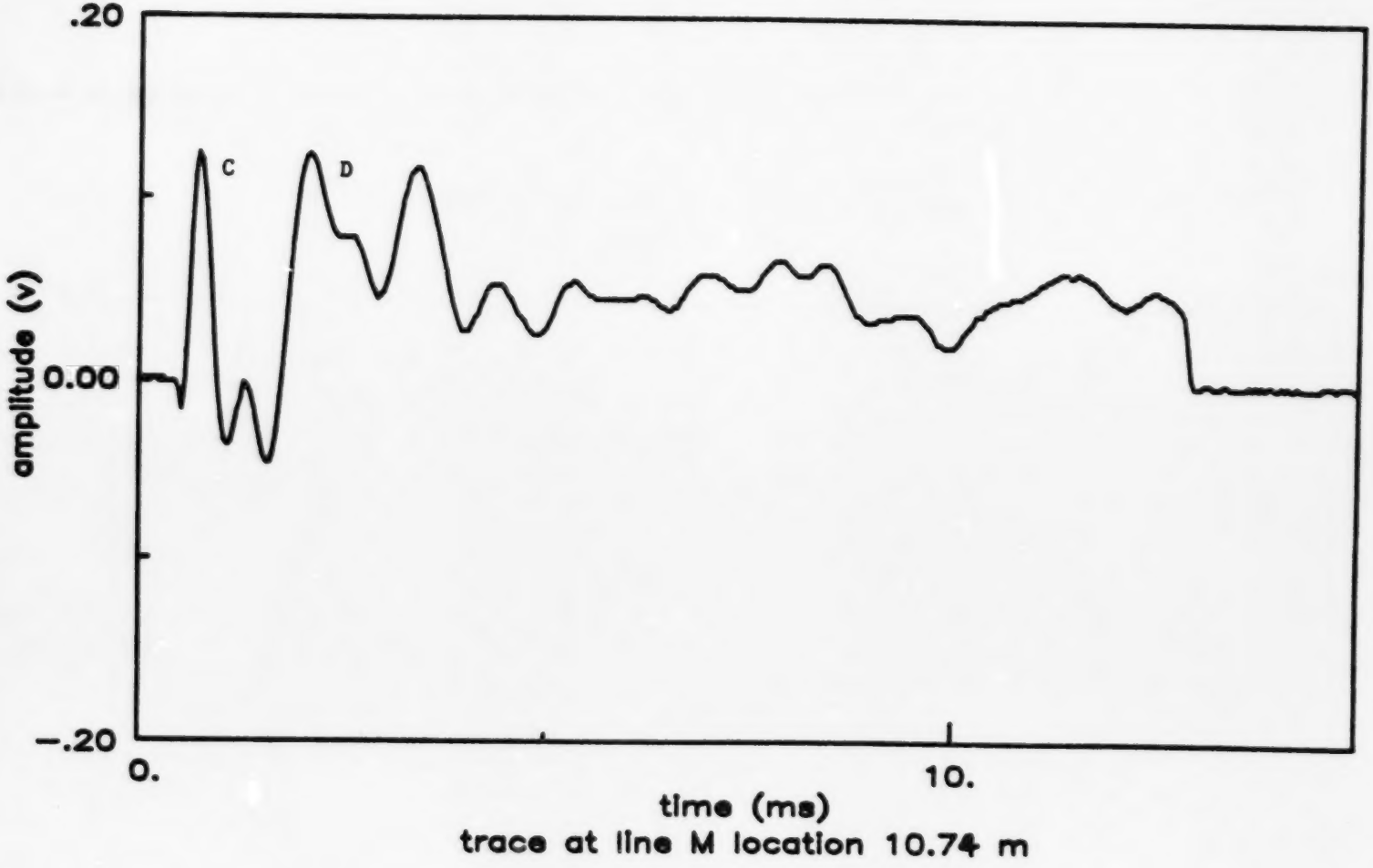

Figure 7/ Gated Video for a Region with No Defects

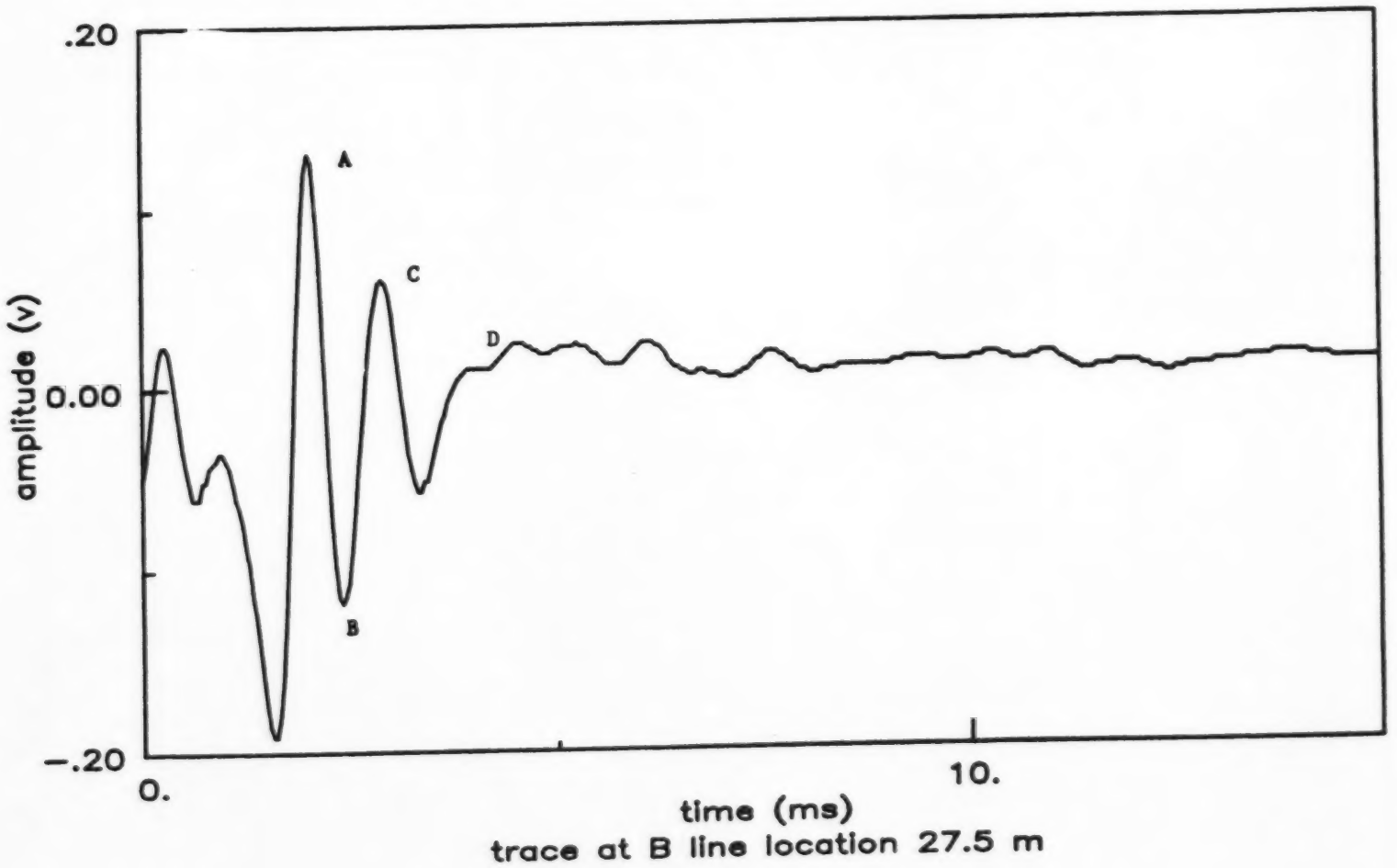

Figure 8/ High Video for a Region with Severe Scaling

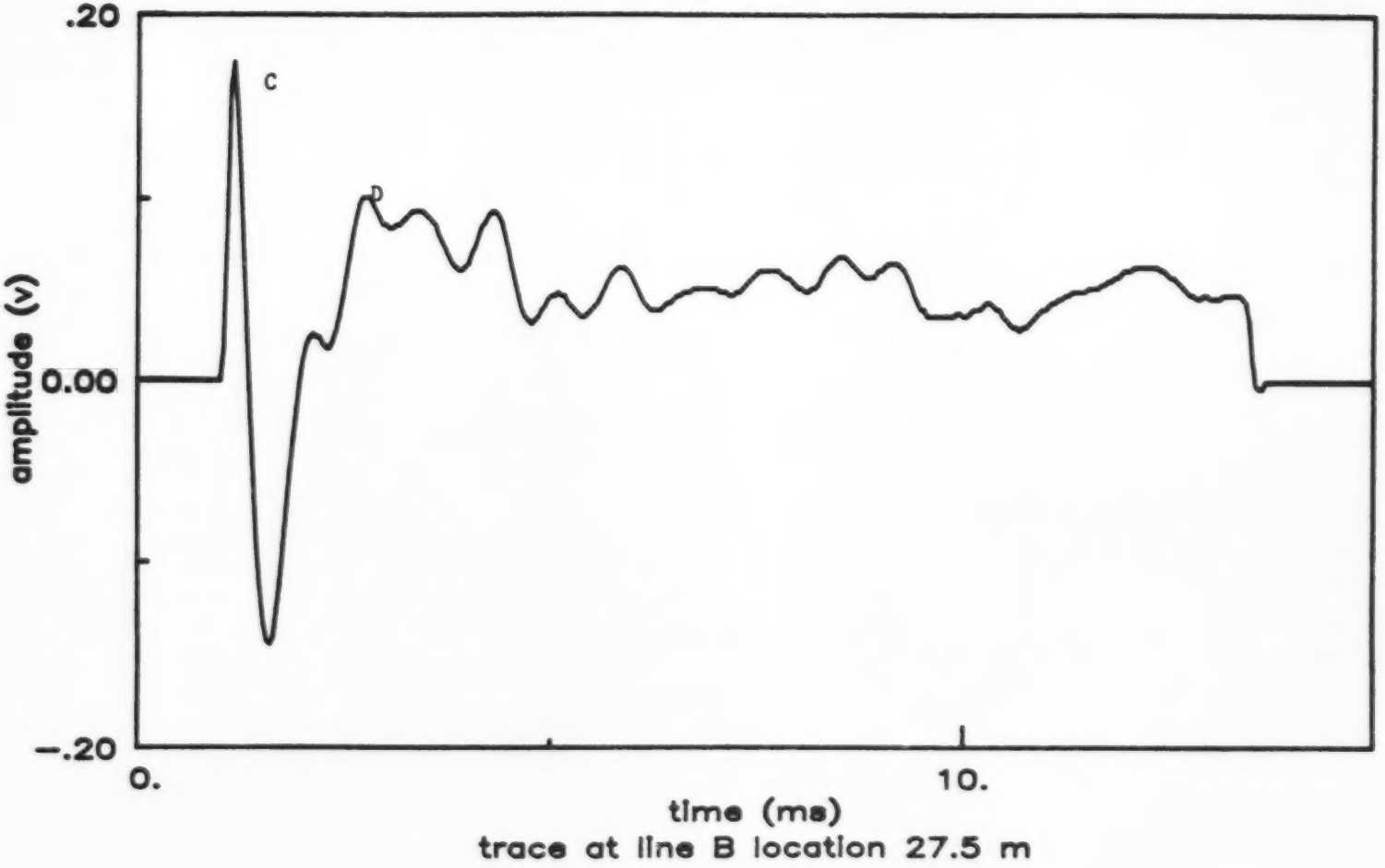

Figure 9/ Gated Video for a Region with Severe Scaling

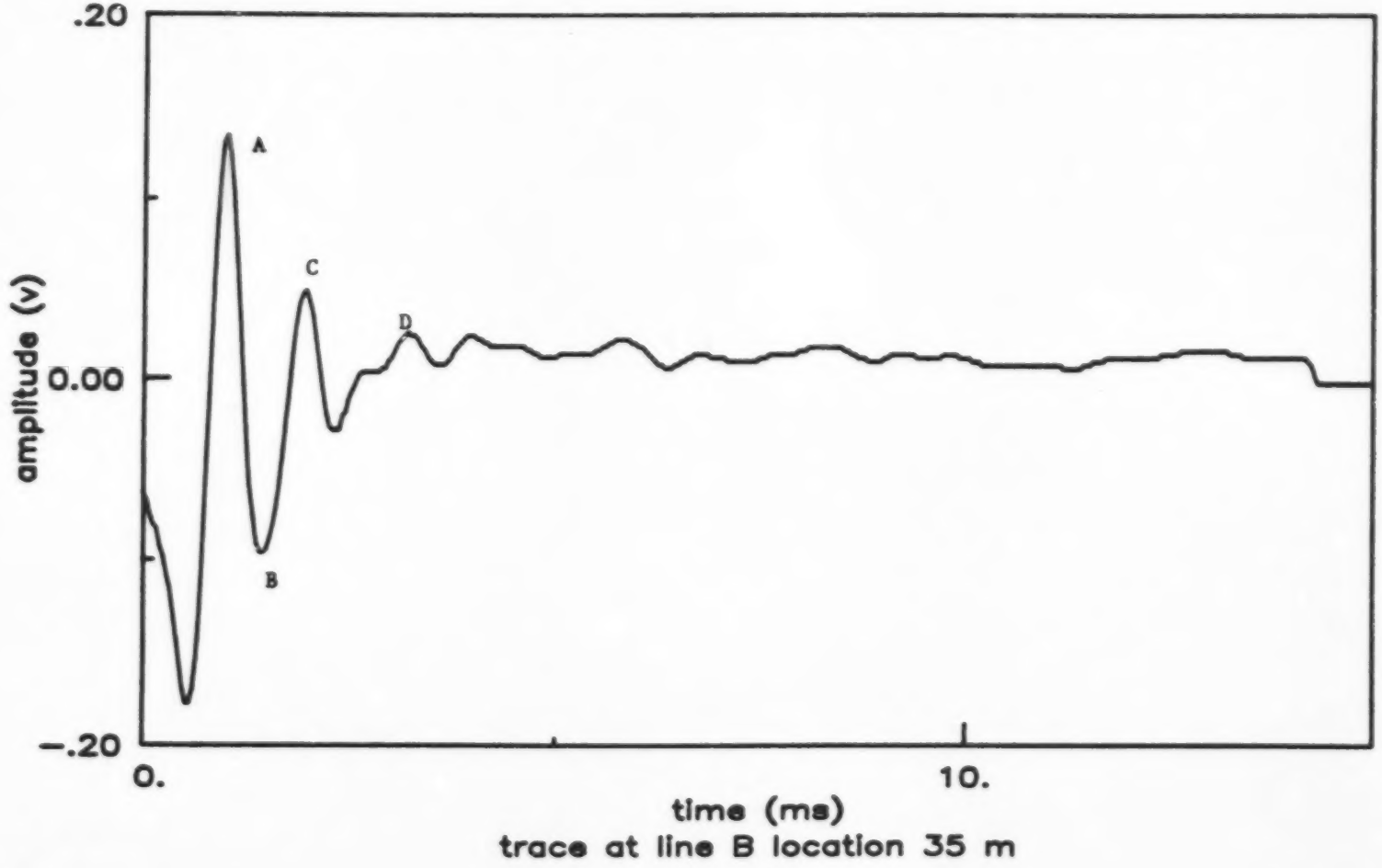

Figure 10/ High Video for a Region with Debonding

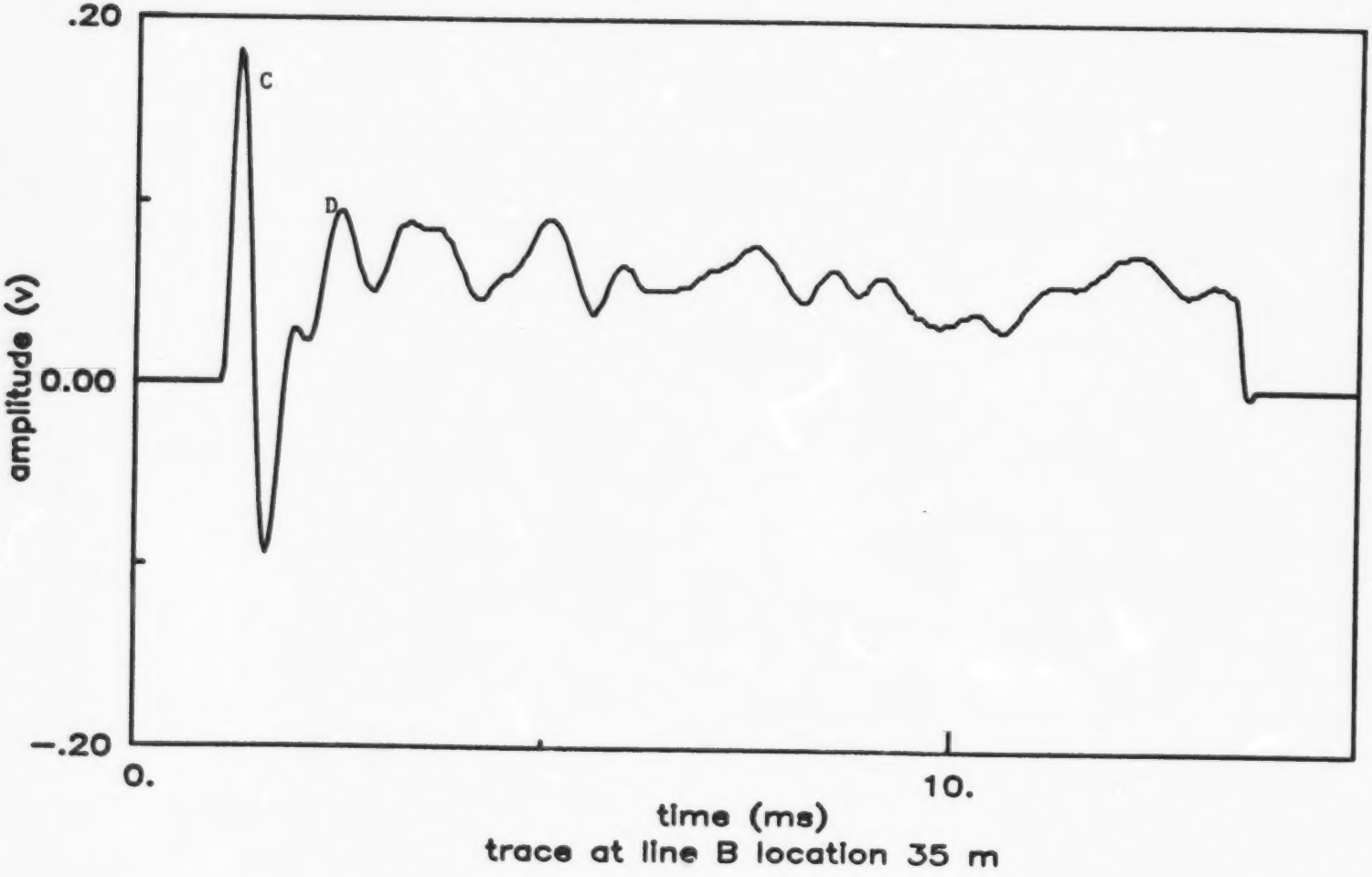

Figure 11/ Gated Video for a Region with Debonding

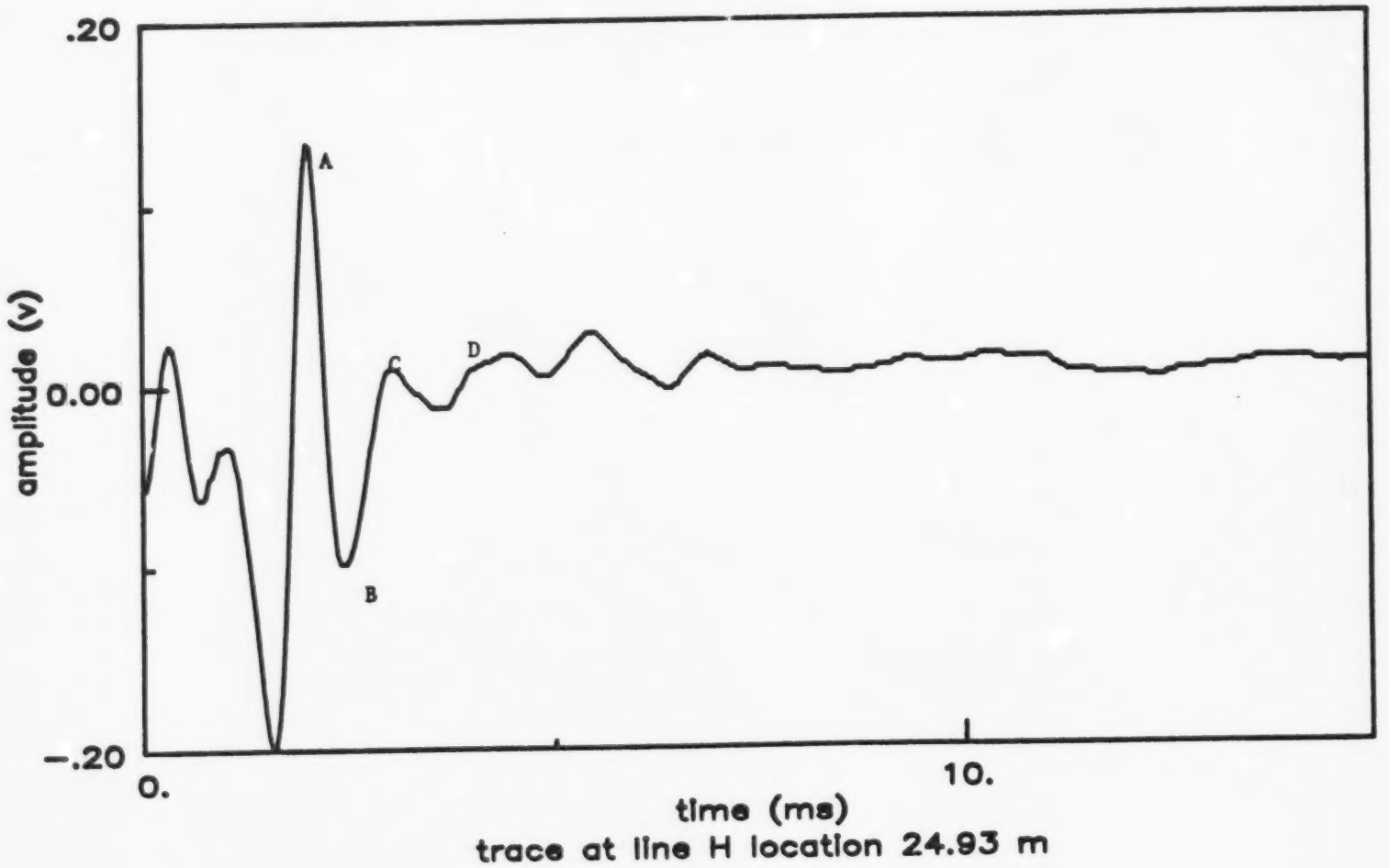

Figure 12/ High Video for a Region with Delamination

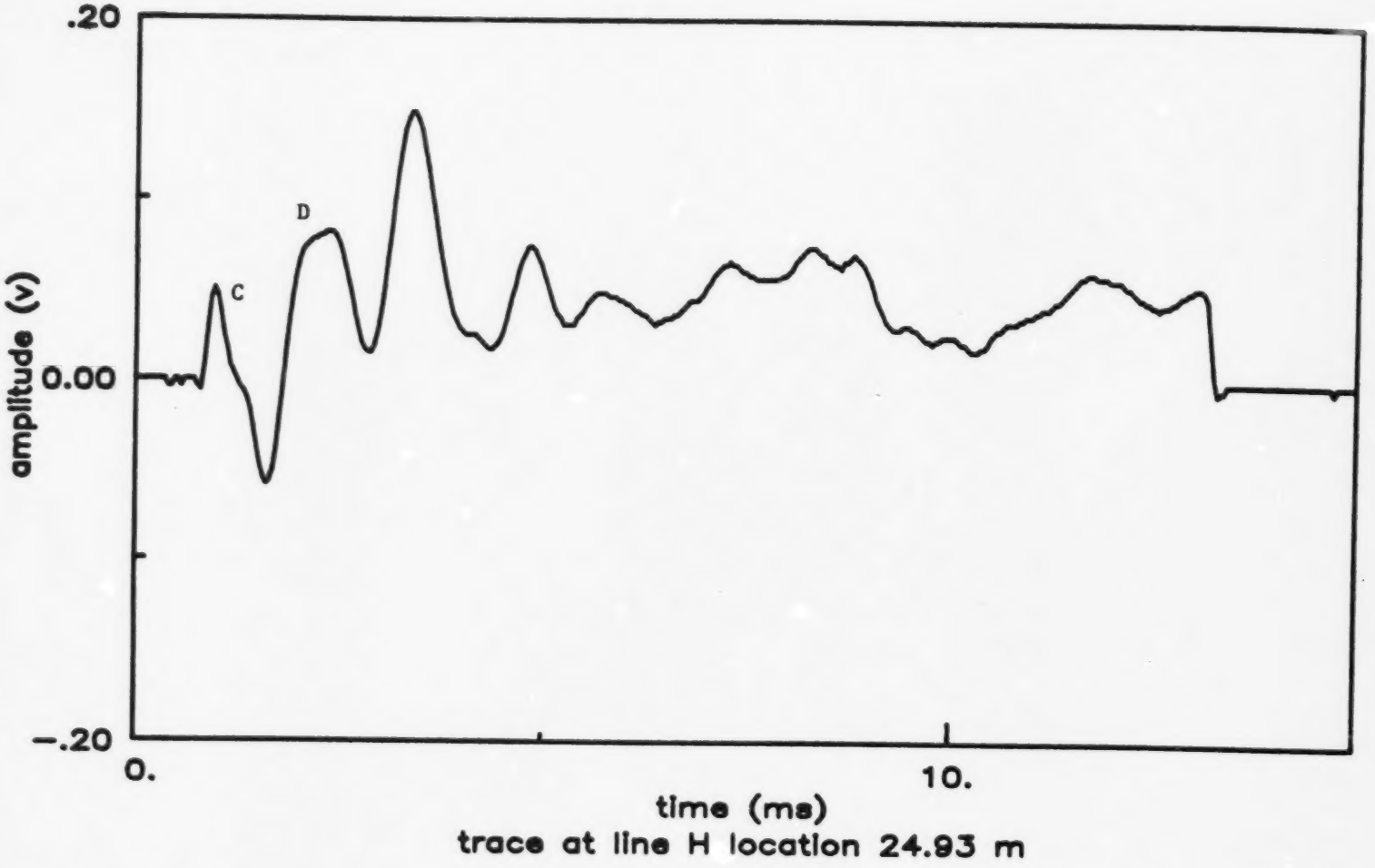

Figure 13/ Gated Video for a Region with Delamination

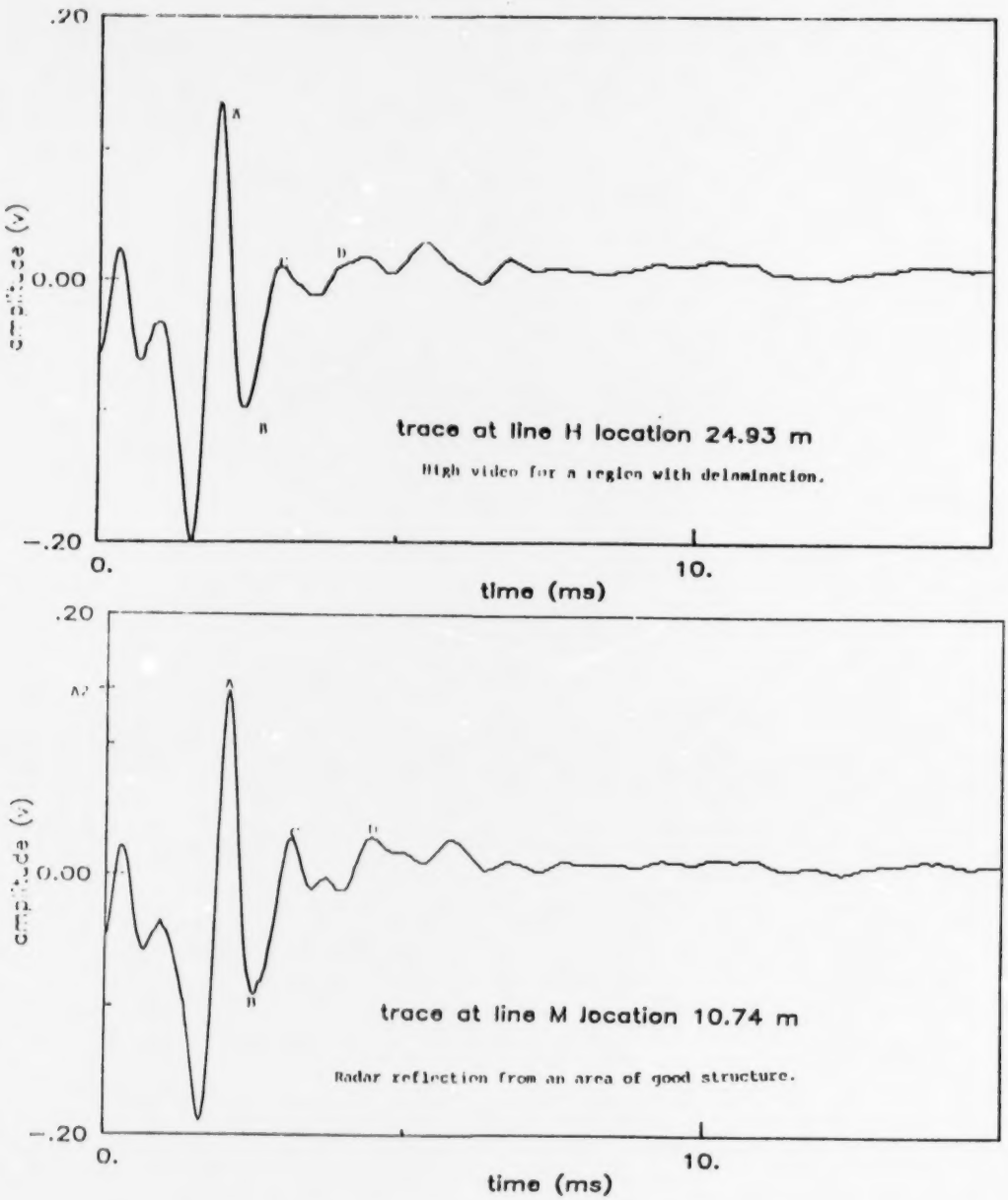

Figure 14/ High Video Comparison

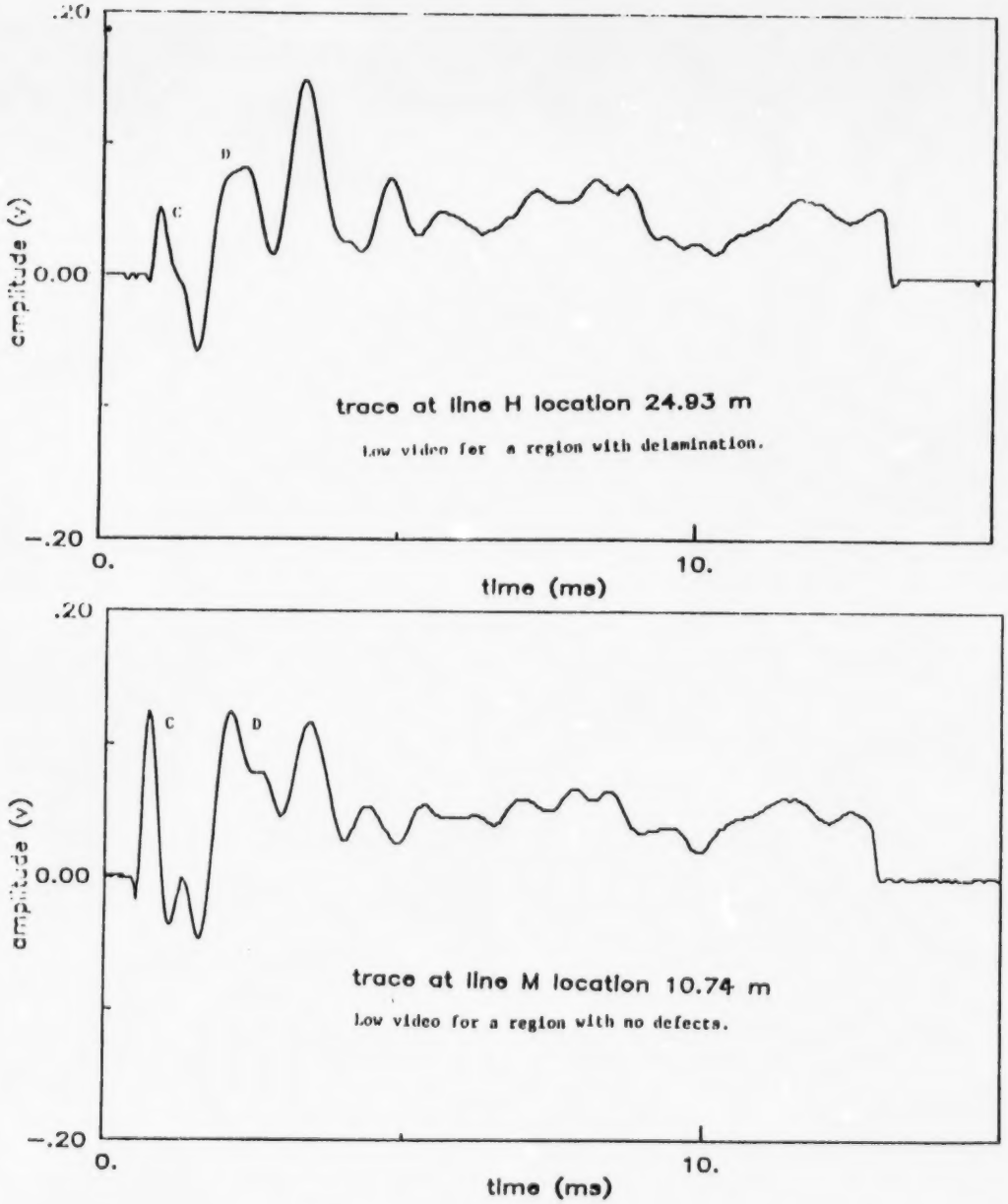

Figure 15/ Gated Video Comparison

Program: DEPTH

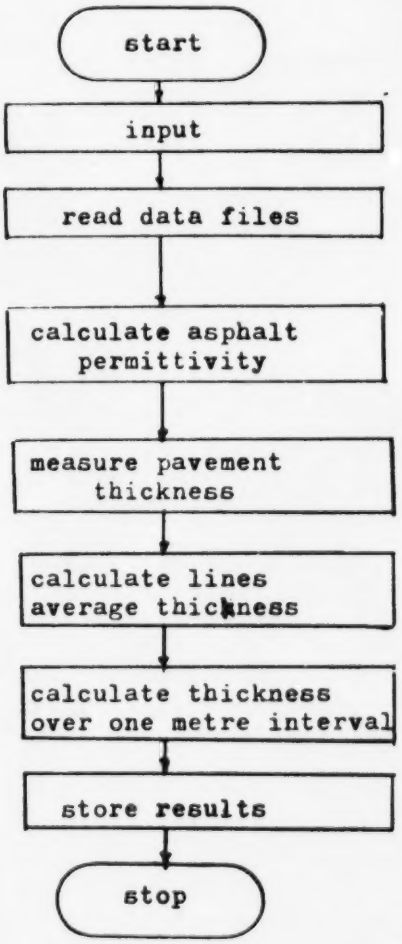

(A)

Program: TABLE

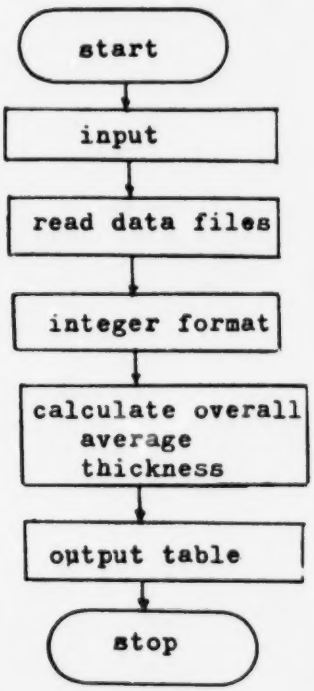

(B)

Figure 16a/ Program for Calculating Asphalt Thickness

16b/ Program for Generating the Printout of Asphalt Thickness

table for the average depth (mm) on the basis of one metre interval

Papineau Creek Bridge Deck
Traveling direction is from South end joint to North end joint
Each grid line is 0.5 metre apart
Date: October 31, 1983

m	B	C	D	E	F	G	H	I	J	K	L	M	N	O	P	Q	R
37	84	102	114	118	118	97	90	83	81	91	101	89	91	94	101	83	92
36	82	91	119	116	111	103	101	94	89	93	94	89	86	95	88	87	107
35	82	105	119	115	111	106	103	96	88	91	92	85	86	88	87	80	78
34	75	114	119	116	112	107	105	96	84	89	89	86	84	84	83	82	72
33	74	115	116	114	111	107	107	98	86	89	91	86	83	80	79	77	79
32	83	112	113	112	106	99	99	91	84	92	93	88	83	80	77	78	90
31	88	112	111	109	102	97	97	89	81	95	94	89	86	82	78	77	74
30	71	106	105	103	101	97	100	93	83	93	93	93	90	82	79	77	71
29	72	101	100	98	96	95	96	91	77	83	85	83	82	78	77	77	71
28	72	99	98	98	94	91	91	85	79	83	84	81	81	77	76	75	71
27	59	94	97	98	96	94	98	89	81	86	88	85	86	78	76	74	70
26	57	90	91	91	92	91	91	91	81	93	97	90	84	76	77	74	85
25	70	78	88	86	86	82	84	85	84	92	90	88	82	76	73	72	92
24	82	88	83	85	82	79	79	87	87	99	94	90	83	75	73	73	80
23	70	89	87	88	86	83	83	91	88	108	102	92	87	80	79	75	71
22	69	90	88	89	88	87	86	88	83	103	102	96	90	82	78	74	70
21	66	88	86	86	87	84	86	84	81	92	95	89	88	84	79	76	69
20	61	90	88	88	84	83	85	81	80	88	88	85	85	84	79	83	70
19	63	85	89	87	86	84	86	80	76	84	85	84	85	83	80	89	69
18	70	84	88	84	83	81	82	80	74	83	82	80	80	77	75	88	66
17	65	87	86	85	81	80	80	76	74	86	83	80	79	75	73	70	64
16	83	85	84	81	81	79	79	77	74	83	82	77	76	74	71	74	67
15	86	95	84	83	80	79	79	77	76	84	80	76	75	72	69	70	69
14	87	91	88	91	85	85	85	81	79	85	82	79	80	76	73	74	65
13	67	90	96	95	93	91	90	86	81	87	85	81	84	81	76	81	60
12	61	86	95	95	91	89	92	86	84	91	89	86	88	86	79	67	54
11	60	84	92	90	87	85	86	85	85	91	90	89	90	86	78	66	53
10	63	81	91	92	90	89	89	87	88	97	97	94	94	92	84	72	54
9	63	81	93	92	92	91	95	93	91	102	106	103	105	103	81	76	63
8	82	87	91	92	91	90	95	92	92	113	115	111	112	115	68	78	77
7	82	88	90	90	91	91	94	90	93	113	115	112	112	108	94	85	76
6	74	93	93	94	92	92	94	88	93	114	115	112	117	115	98	82	75
5	67	98	97	97	94	89	91	90	88	101	108	100	111	116	79	83	79
4	69	108	99	96	92	88	86	83	80	91	99	98	104	80	77	79	80
3	72	110	102	94	90	85	83	78	75	87	95	96	100	111	74	81	76
2	77	96	92	88	91	86	92	76	71	82	85	87	89	91	82	86	68
1	***	***	96	95	***	76	***	71	66	76	91	85	86	90	115	86	83
0																	
AVE	72	93	96	95	93	90	90	86	82	92	93	90	89	86	79	78	73

OVERALL AVERAGE DEPTH = 86

Figure 17/ Depth of Asphalt Printout

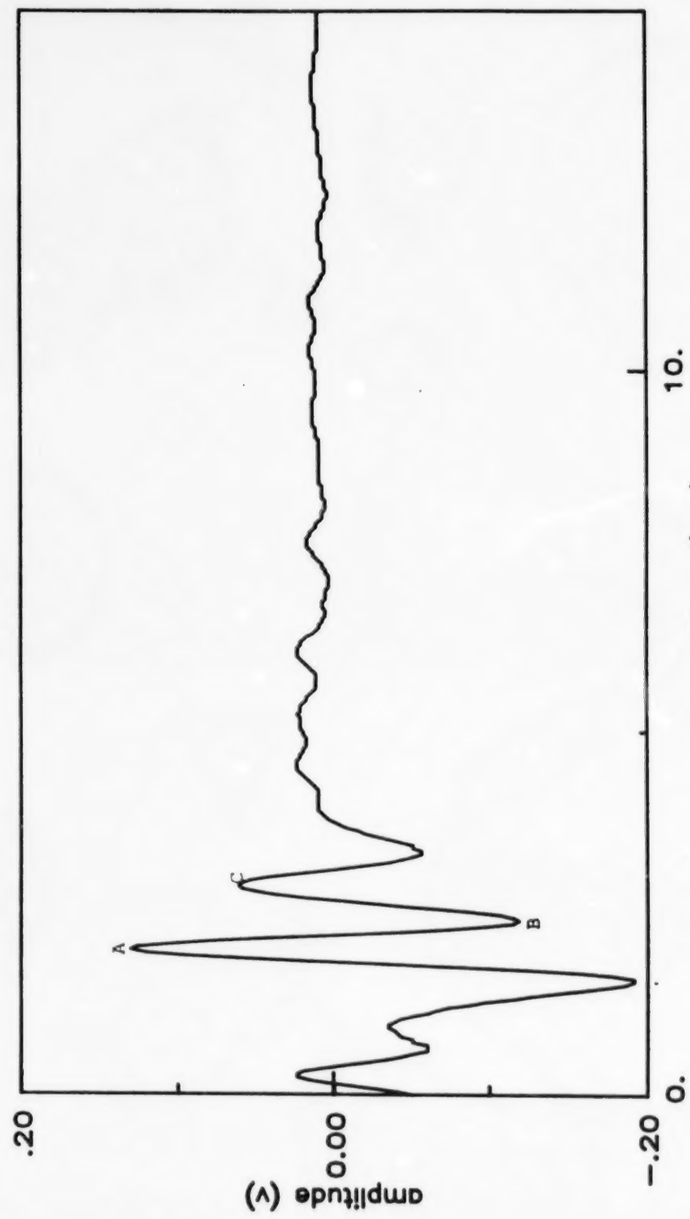

Figure 18/ Waveform Showing Scaling
Note the Amplitudes at Point B and C Relative to Point A.

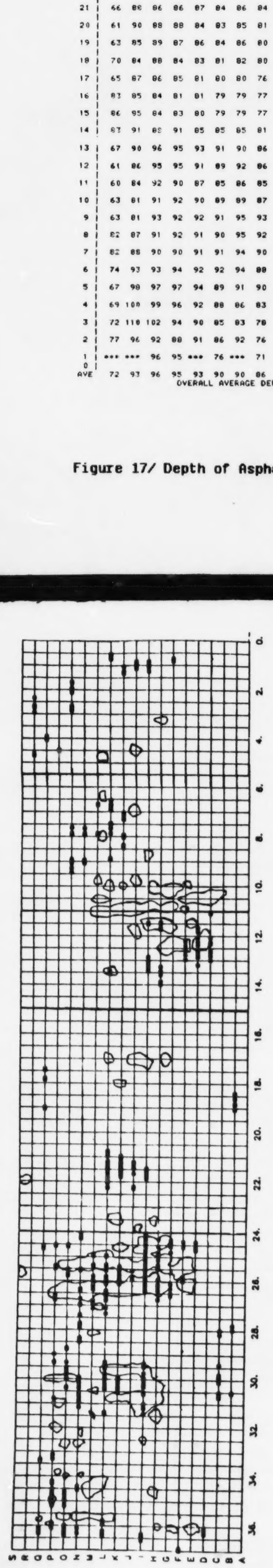

Figure 31/ Papineau Creek Comparing the Actual Delaminated Areas with the Computer Results

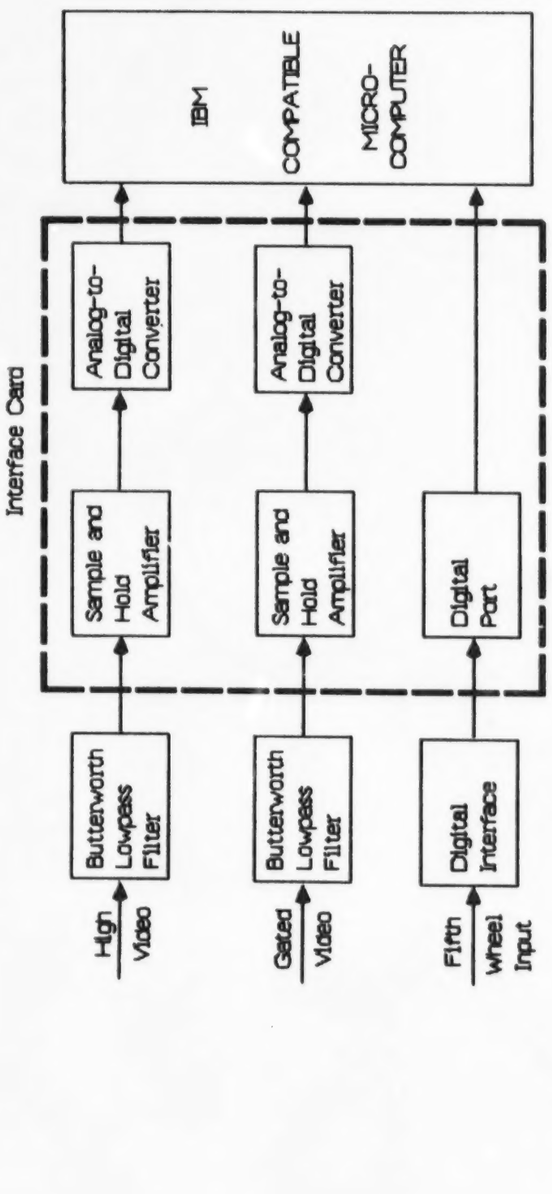

Figure 32/ Block Diagram of the Sampling and Digitizing System

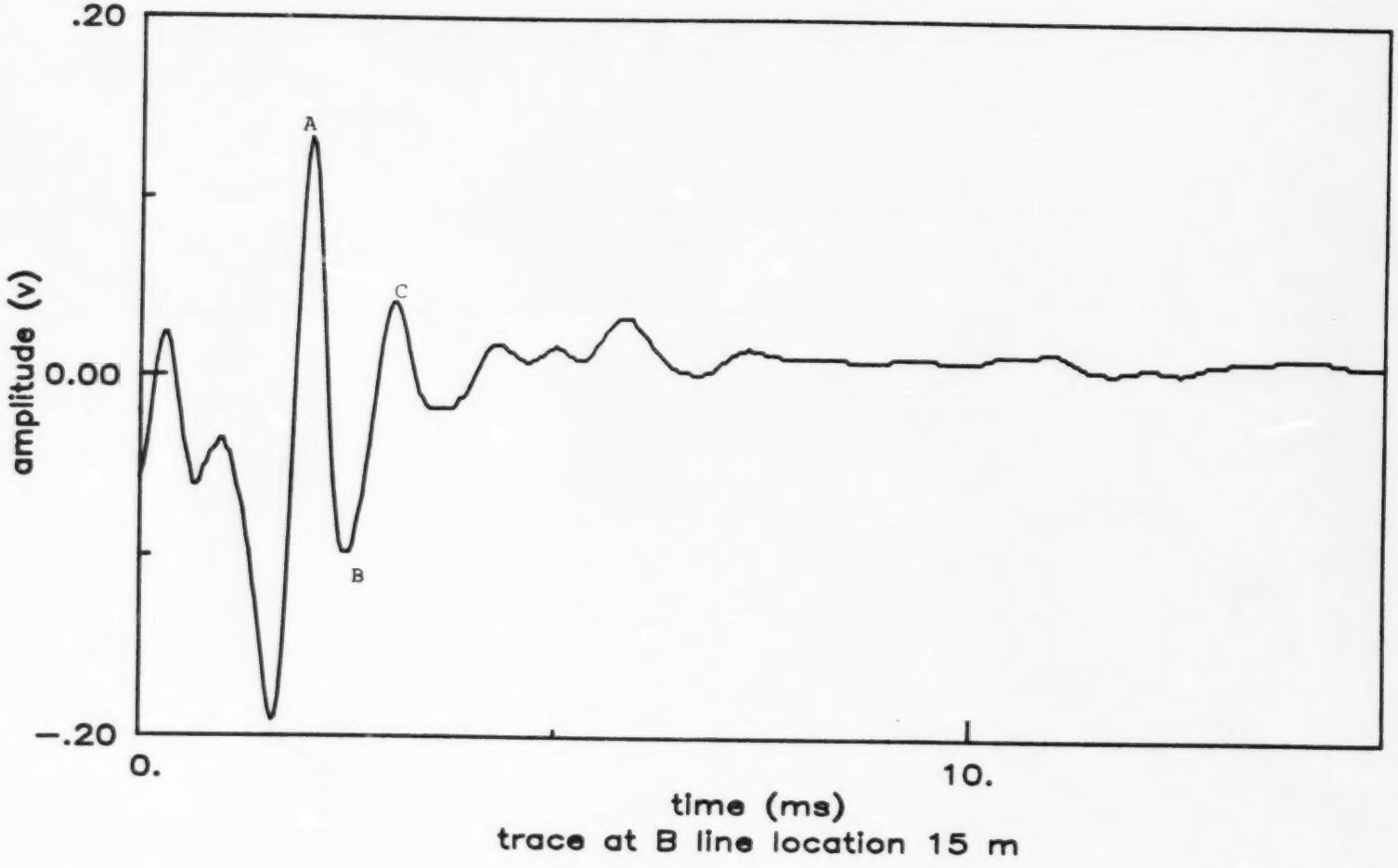

Figure 19/ Waveform Showing Debonding

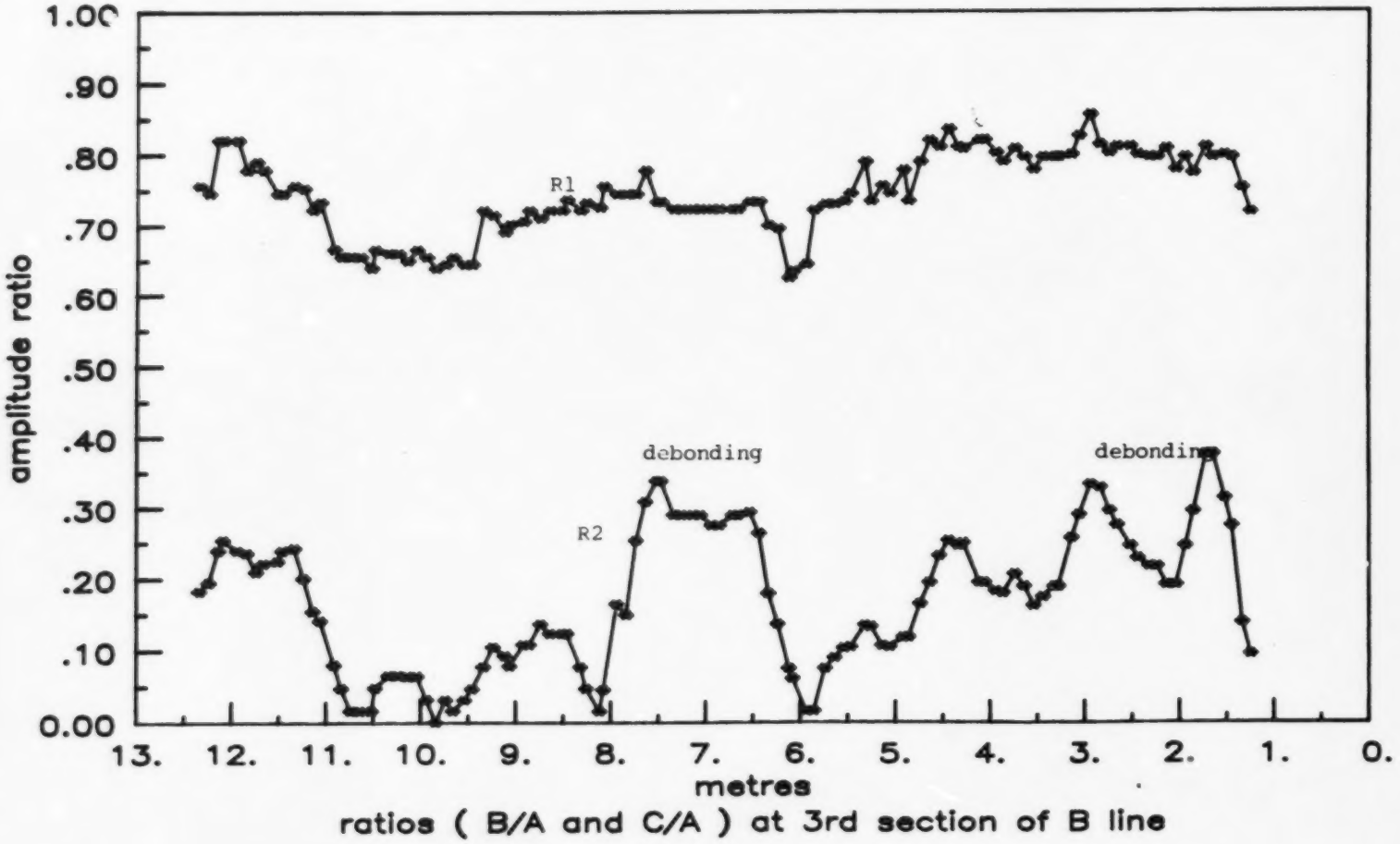

Figure 20/ Plot of Ratio R1 and R2 for the B Line
Note the Regions of Debonding.

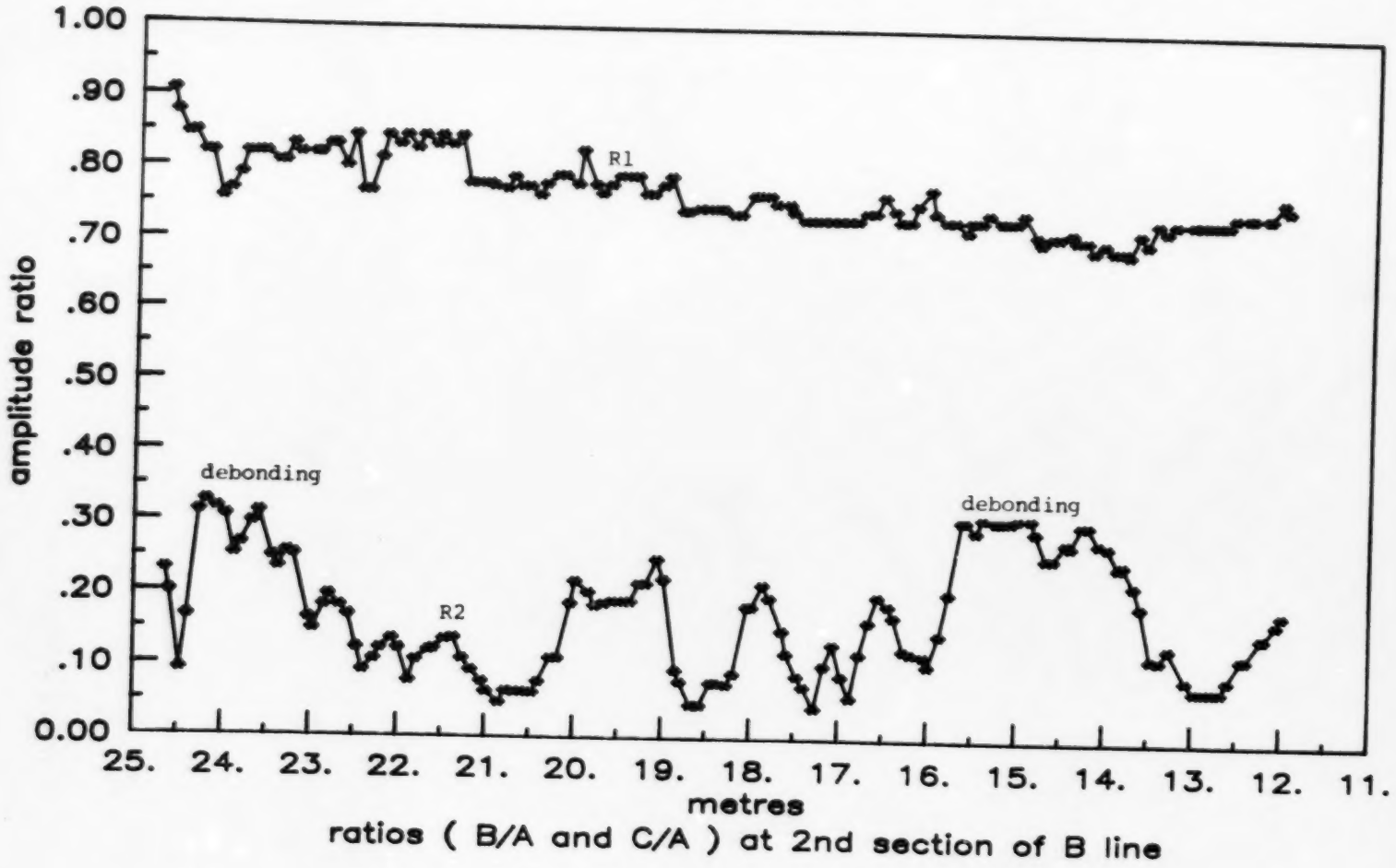

Figure 21/ Plot of Ratio R1 and R2 for the B Line
Note the Regions of Debonding.

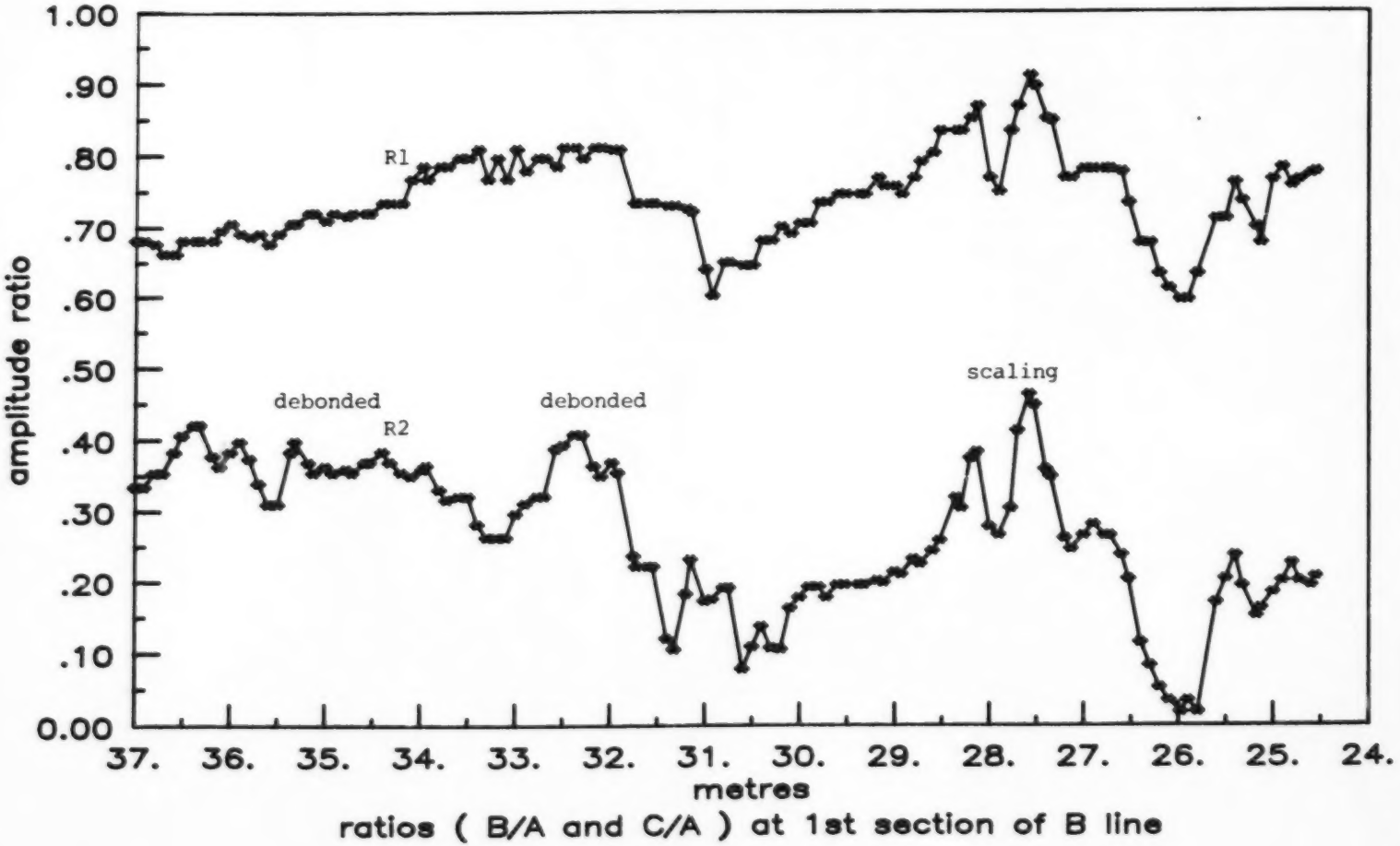

Figure 22/ Plot of Ratio R1 and R2 for the B Line
Note the Regions of Debonding and Scaling.

Subroutine: R1R2

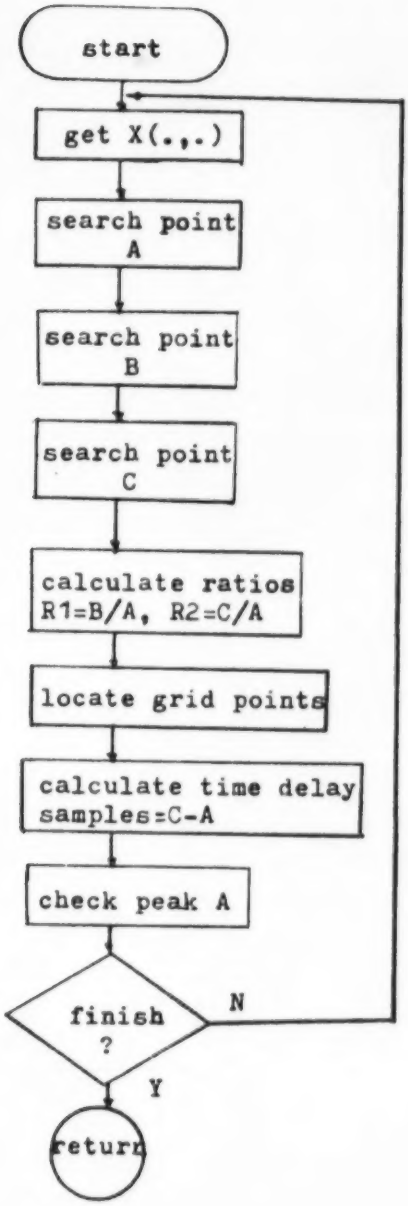

(A)

Subroutine: OXING

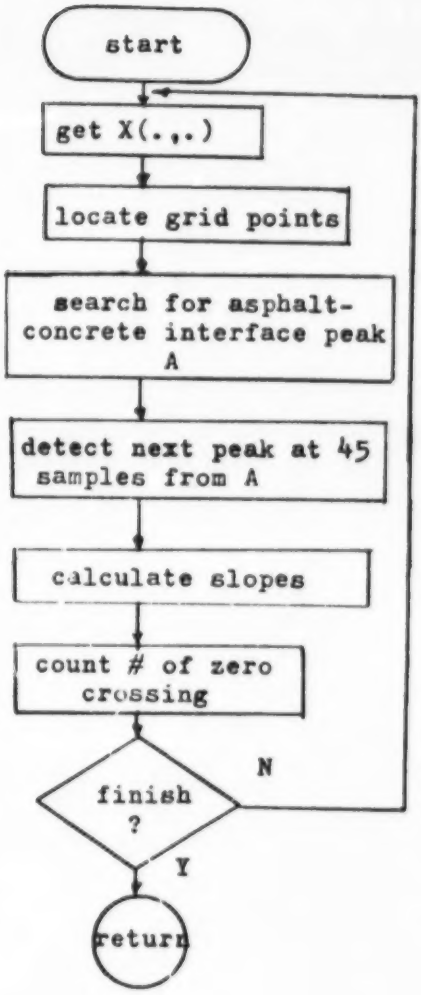

(B)

Figure 23a/ Flow Chart of the Ratio Test

23b/ Flow Chart of the Zero Crossing Subroutine

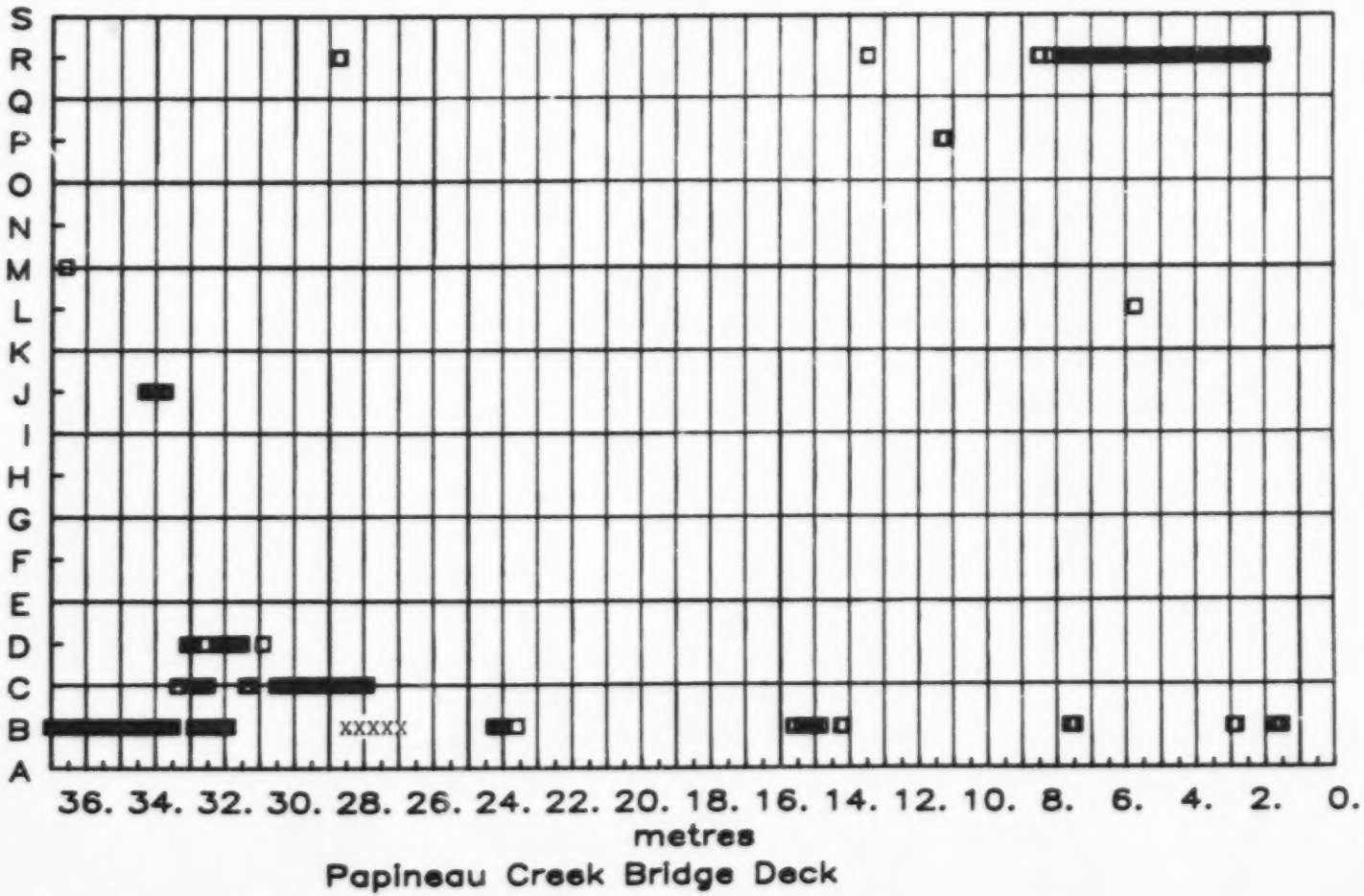

Figure 24/ Areas of Debonding and Scaling
Debonding is Marked with '□' while Scaling is Indicated with 'X'.

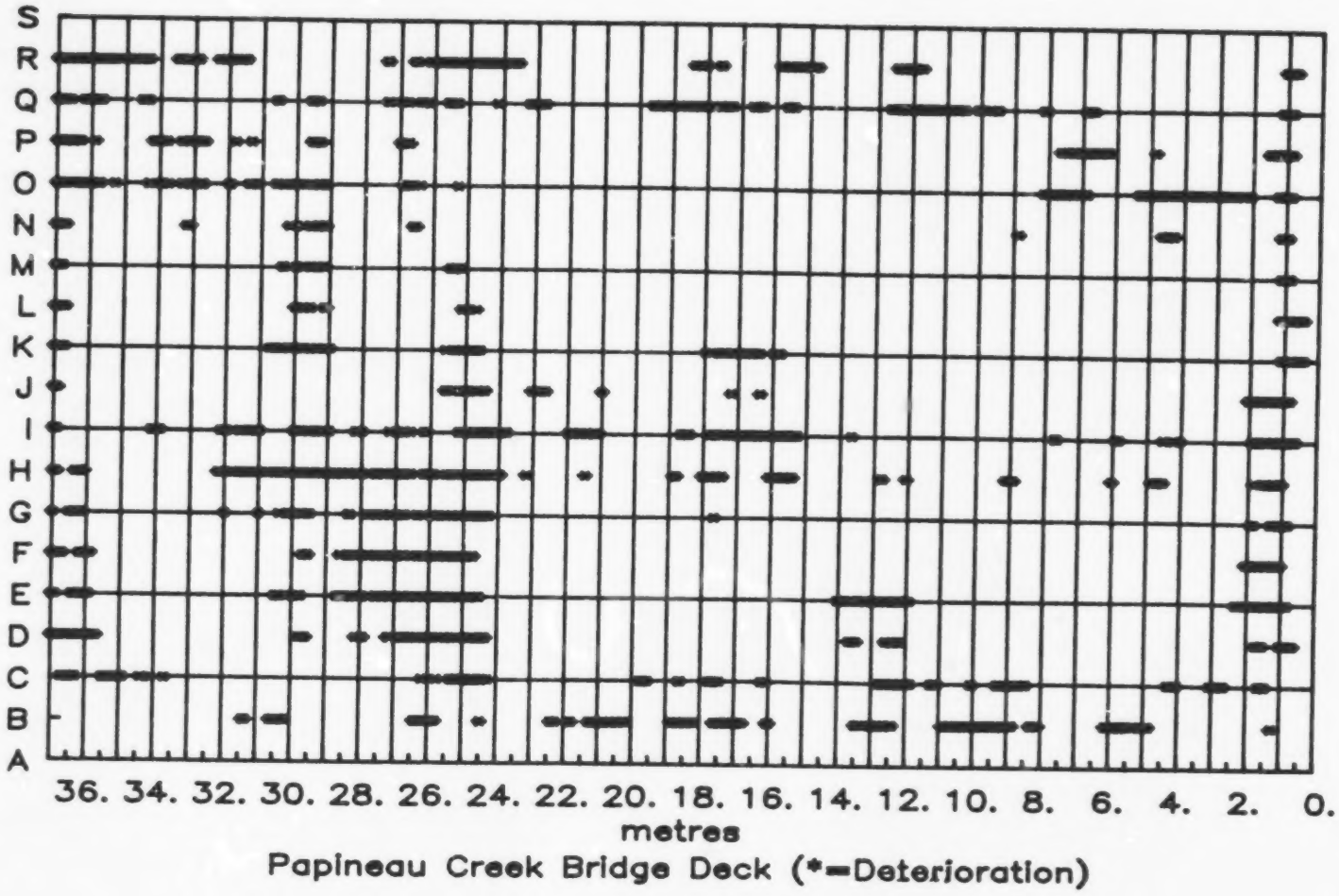

Figure 25/ Plot of the Bridge Deck Using the Ratio Test
Note the Large Number of False Alarms.

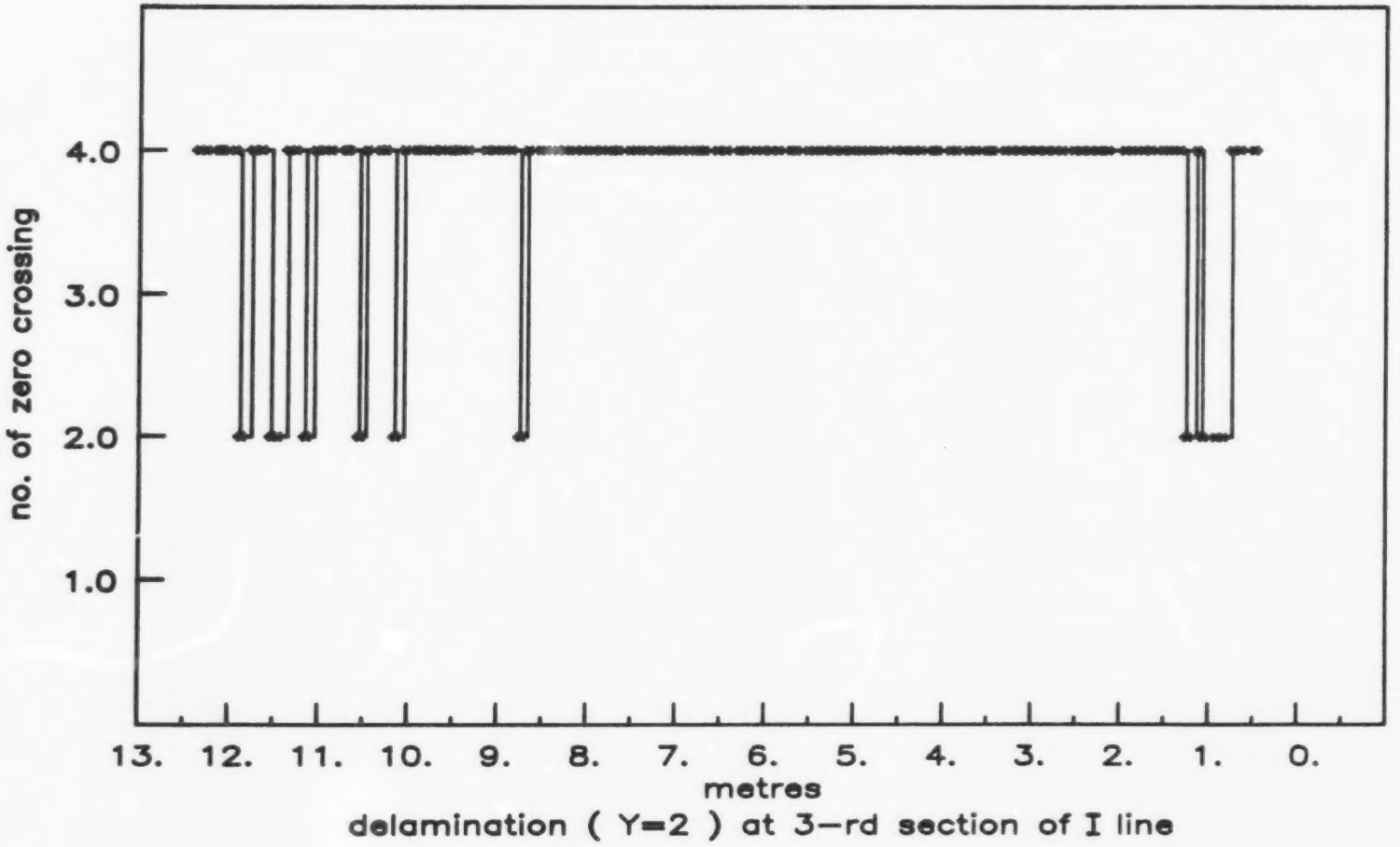

Figure 26/ Plot of Sign Changes for the I Line

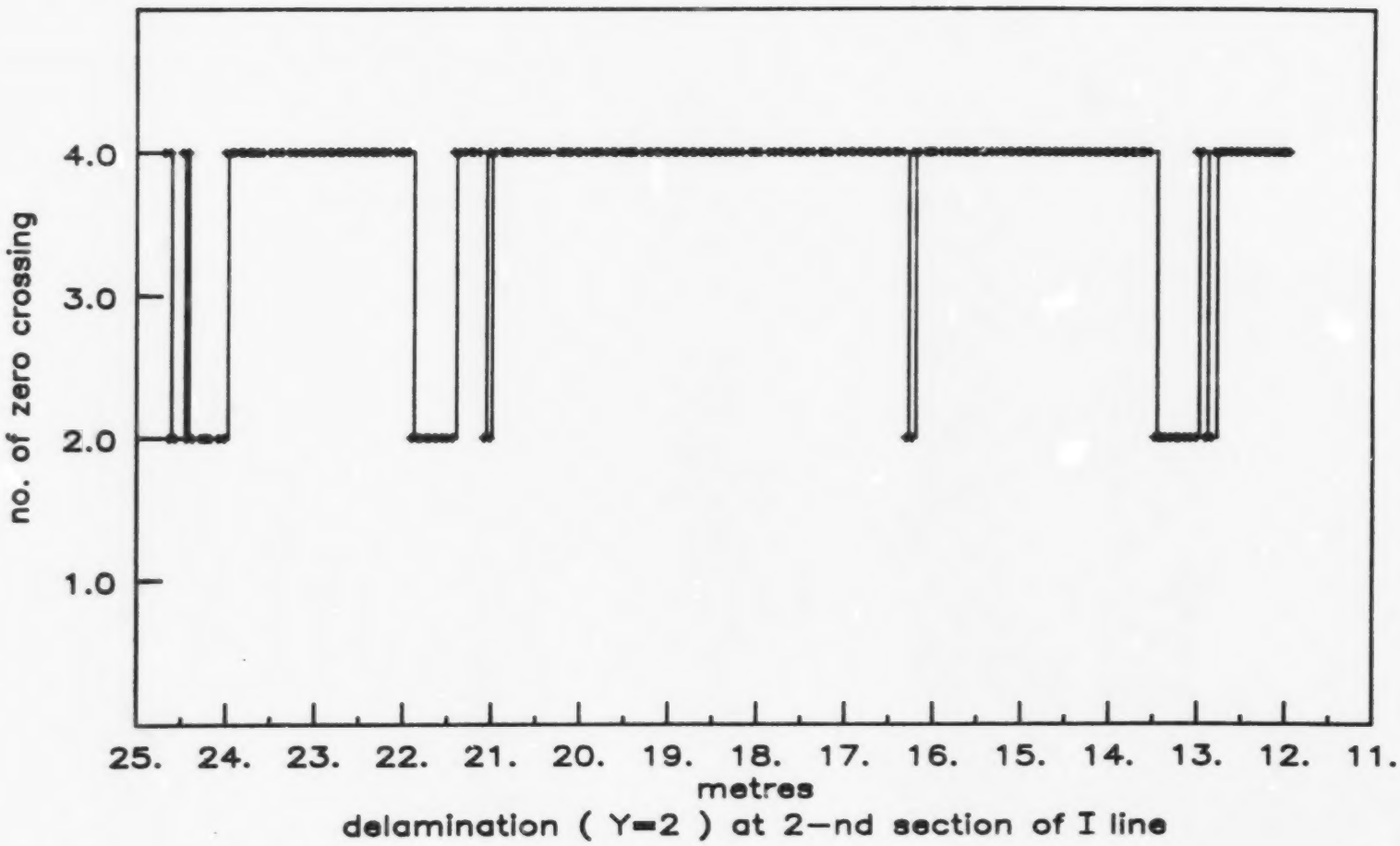

Figure 27/ Plot of Sign Changes for the I Line, Continued

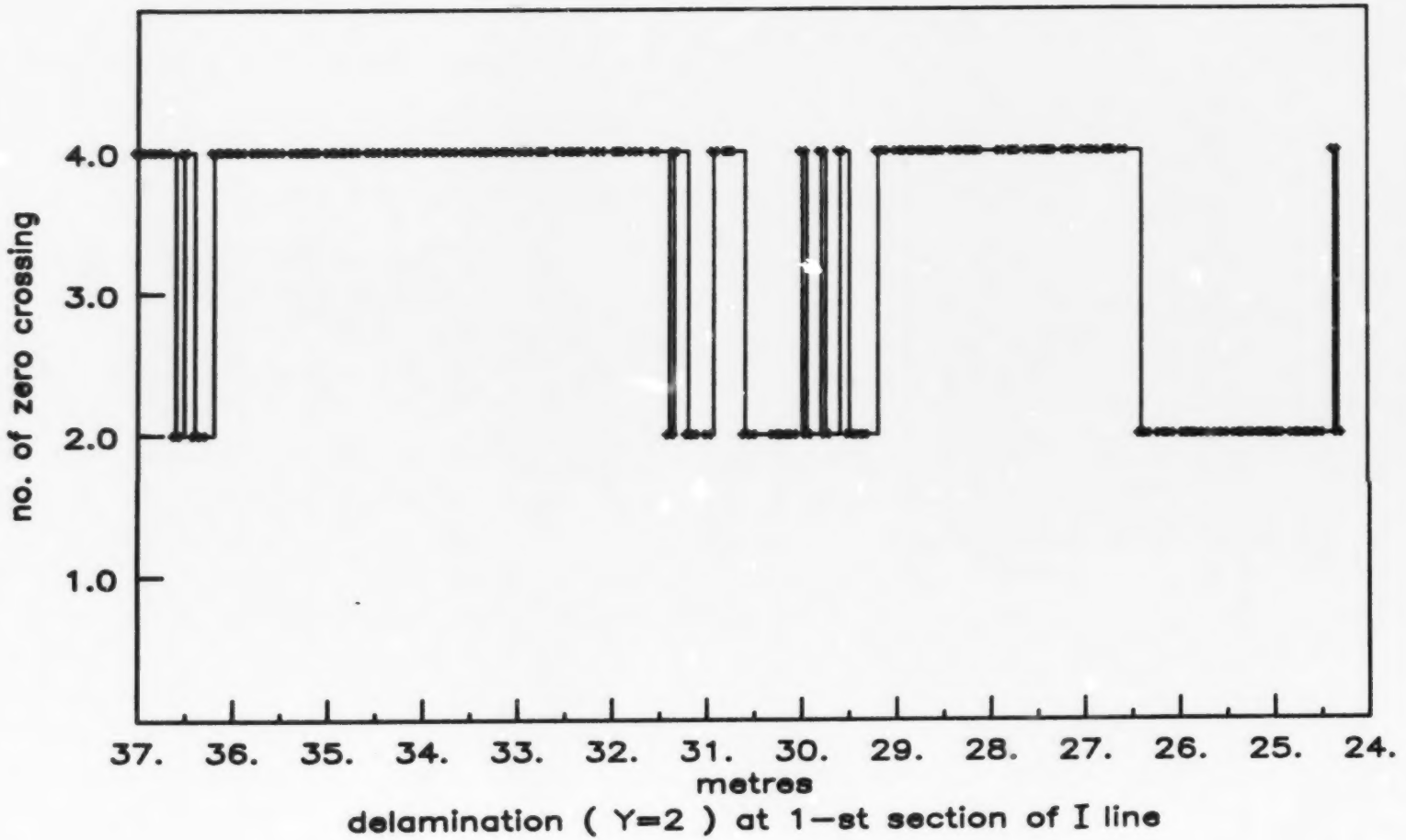

Figure 28/ Plot of Sign Changes for the I Line, Continued

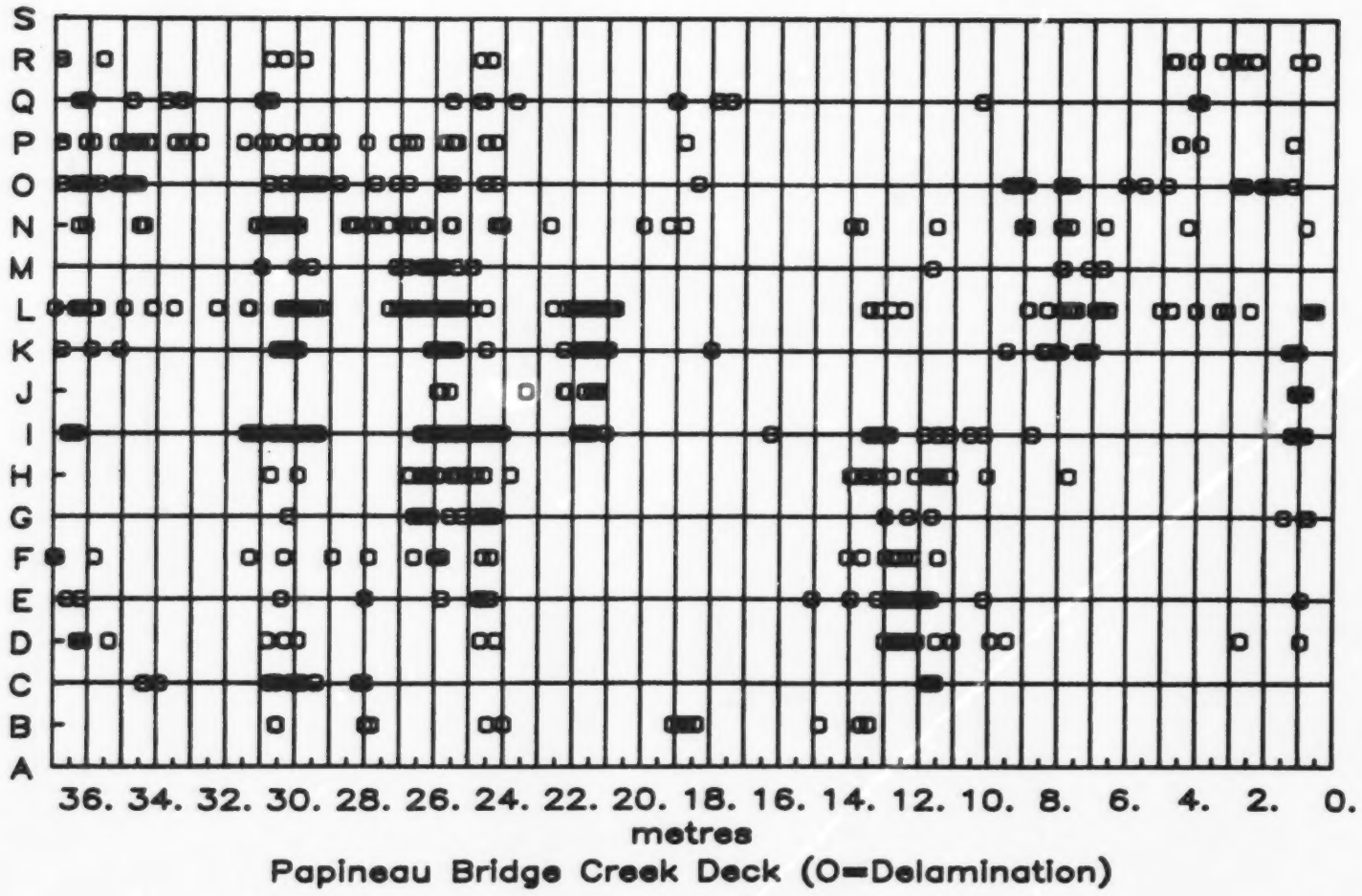

Figure 29/ Plot of Areas of Delamination

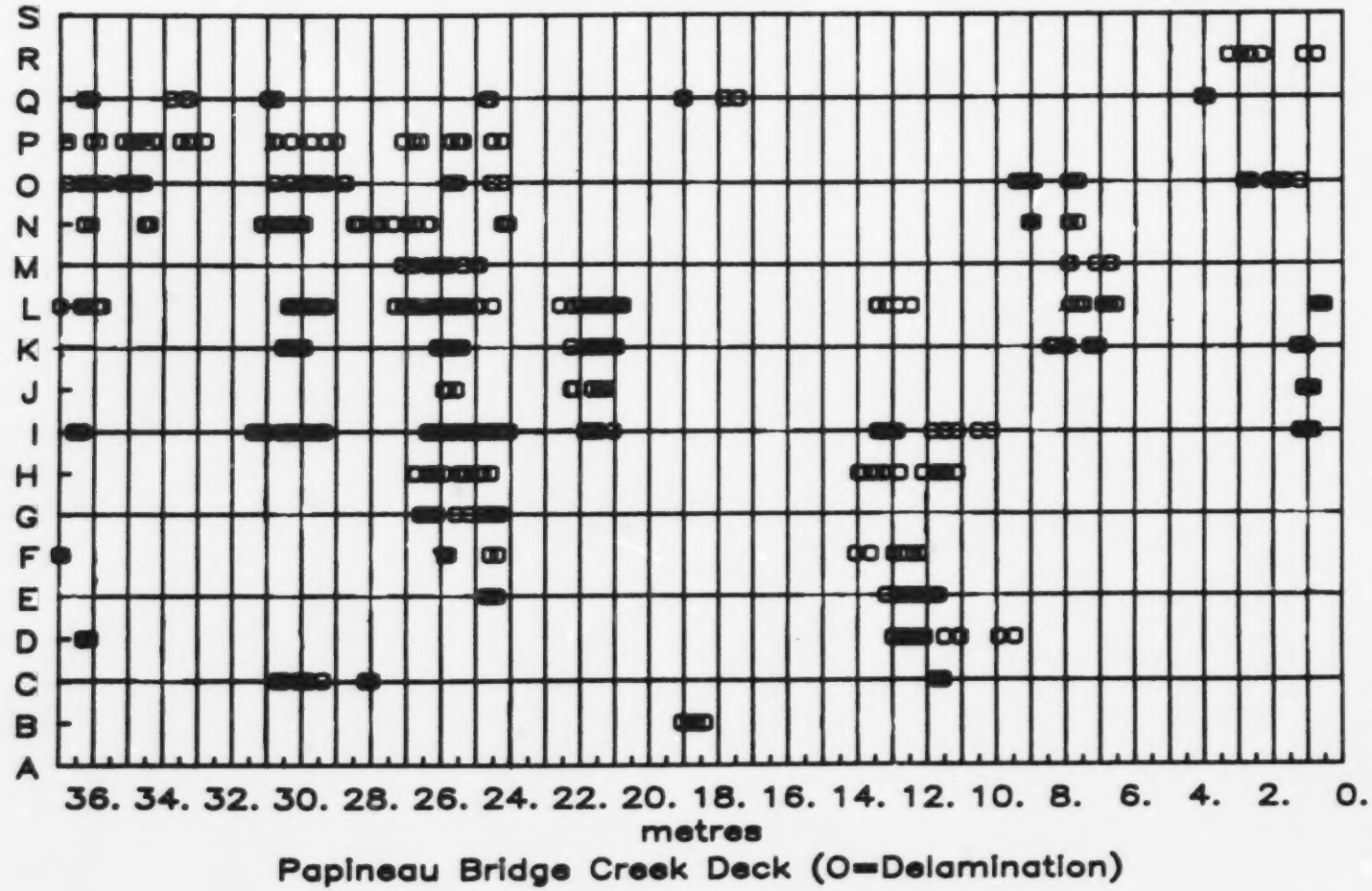

Figure 30/ Plot of Areas of Delamination
Note Single Hits Indication are Eliminated

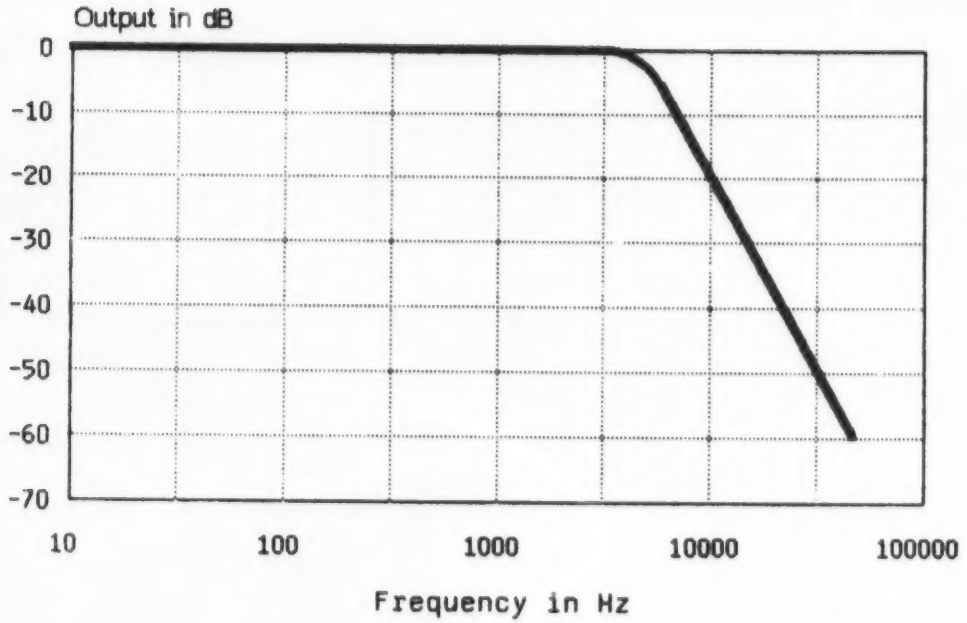

Figure 33/ Frequency Response

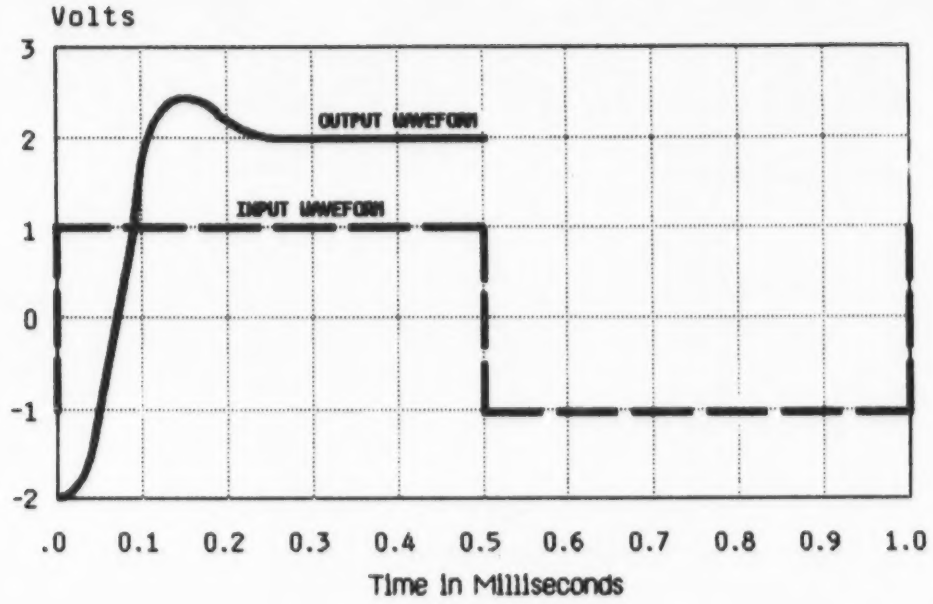

Figure 34/ Transient Response

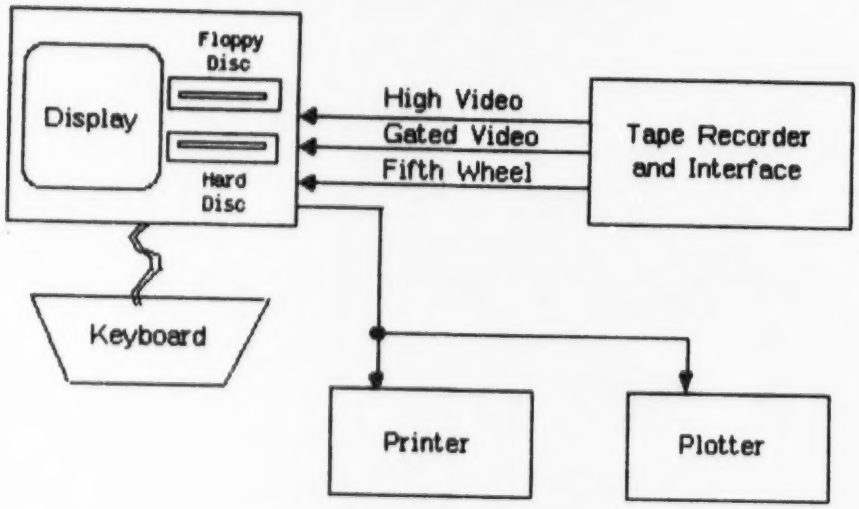

Figure 35/ Overall Block Diagram of the System